

# Singular diffusionless limits of double-diffusive instabilities in magnetohydrodynamics

Oleg N. Kirillov <sup>1,2</sup>

<sup>1</sup>Steklov Mathematical Institute, Russian Academy of Sciences, Gubkina 8, Moscow 119991, Russia, E-mail: kirillov@mi.ras.ru

<sup>2</sup>Universita di Trento, DICAM, via Mesiano 77, I-38123 Trento, Italy, E-mail: oleg.kirillov@unitn.it

## Abstract

We study local instabilities of a differentially rotating viscous flow of electrically conducting incompressible fluid subject to an external azimuthal magnetic field. In the presence of the magnetic field the hydrodynamically stable flow can demonstrate the azimuthal magnetorotational instability (AMRI) both in the diffusionless case and in the double-diffusive case with viscous and ohmic dissipation. Performing stability analysis of the amplitude transport equations of the short-wavelength approximation, we find that the threshold of the diffusionless AMRI via the Hamilton-Hopf bifurcation is a singular limit of the thresholds of the viscous and resistive AMRI corresponding to the dissipative Hopf bifurcation and manifests itself as the Whitney umbrella singular point. A smooth transition between the two types of instabilities is possible only if the magnetic Prandtl number is equal to unity,  $Pm = 1$ . At a fixed  $Pm \neq 1$  the threshold of the double-diffusive AMRI is displaced by an order one distance in the parameter space with respect to the diffusionless case even in the zero dissipation limit. The complete neutral stability surface contains three Whitney umbrella singular points and two mutually orthogonal intervals of self-intersection. At these singularities the double-diffusive system reduces to a marginally stable system which is either Hamiltonian or parity-time (PT) symmetric.

## 1 Introduction

While common sense tends to assign to dissipation the role of a vibration damper, as early as 1879 Kelvin and Tait presented a class of Hamiltonian equilibria, which, being stable in the absence of dissipation, become unstable due to action of dissipative forces [9, 31]. The universality of the *dissipation-induced instabilities* manifests itself in unexpected links between solid- and fluid mechanics [41, 13, 26, 29]. For instance, destabilizing action of viscous dissipation on the negative energy mode of rotation of a particle moving in a rotating cavity [33] selects the backward whirling in the rotating frame as an unstable (anticyclonic) motion. Remarkably, this very instability mechanism described by Lamb in 1908 has recently re-appeared as a trigger breaking the cyclone-anticyclone vortex symmetry in a rotating fluid in the presence of linear Ekman friction [16]. Especially intriguing the destabilization by dissipation is when several diffusion mechanisms act simultaneously [59, 56]. In this case “no simple rule for the effect of introducing small viscosity or diffusivity on flows that are neutral in their absence appears to hold” [55].

The onset of the classical Hopf bifurcation in a near-Hamiltonian dissipative system generically does not converge to the onset of the Hamilton-Hopf bifurcation of a Hamiltonian system when dissipation tends to zero [34]. In meteorology this phenomenon is known as the “Holopäinen instability mechanism” for a baroclinic flow when waves that are linearly stable in the absence of Ekman friction become dissipatively destabilized in its presence, with the result that the location of the curve of marginal stability is displaced by an order one distance in the parameter space, even if the Ekman number is infinitesimally small [22, 31, 54, 57]. Similar effect in solid mechanics is represented by the “Ziegler destabilization paradox” [60, 26, 11].

In plasma physics and magnetohydrodynamics (MHD) the discrepancy between the stability thresholds of an ideal system and that of the system with vanishing dissipation has even led to a radical conclusion [44]: “A great deal of time was wasted analyzing ideal MHD equilibria which could never be reached as the limit of a resistive equilibrium with small but non-zero resistivity. Much as in the mid-nineteenth century, the point was missed that for fluid equations of the Navier-Stokes type the ideal limit with zero dissipation coefficients has essentially nothing to do with the case of small but finite dissipation coefficients.”

Swaters noticed in [54] that the stability boundary associated with the zero dissipation limit of a dissipative baroclinic instability theory does not collapse to the inviscid result when the Ekman dissipation is replaced by other dissipative mechanisms, e.g. by horizontal turbulent friction, confirming that such a *singular limit* is generic. However, he also managed to choose a specific dissipative perturbation (in which the dissipation is proportional to the geostrophic potential vorticity) possessing coincidence of the zero dissipation limit of the dissipative marginal stability boundary with the inviscid result [54]. In solid mechanics generic character of the discontinuity of the instability threshold in the zero dissipation limit was noticed already in the work by Smith [50, 25] who found that a viscoelastic shaft rotating in bearings with viscous damping is prone to the dissipation-induced instability for almost all *ratios* of the damping coefficient of the shaft and the damping coefficient of the bearings, except one specific ratio.

In hydrodynamics and MHD the ratio of damping coefficients corresponding to different dissipative mechanisms is traditionally called *the Prandtl number*. For example, the Prandtl number,  $\text{Pr} = \nu/\kappa$ , measures the relative strength of the diffusion of vorticity represented in the Navier-Stokes equations by the kinematic viscosity coefficient  $\nu$  and thermal diffusion with the coefficient of thermal diffusivity  $\kappa$  [1]. The magnetic Prandtl number,  $\text{Pm} = \nu/\eta$ , is the ratio of the coefficients of the kinematic viscosity and ohmic diffusion,  $\eta$  [5, 12]. To get an idea of the key role of the Prandtl numbers in the correspondence between stability criteria in the diffusionless and the double-diffusive case let us consider the Rayleigh centrifugal instability criterion and its extensions.

The Rayleigh criterion predicts a stationary axisymmetric instability of an ideal incompressible Newtonian fluid, differentially rotating with the radially-varying angular velocity  $\Omega = \Omega(r)$ , if

$$\text{Ro} + 1 < 0, \tag{1.1}$$

where  $\text{Ro}$  is the fluid Rossby number

$$\text{Ro} := \frac{r\partial_r\Omega}{2\Omega} \tag{1.2}$$

and  $\partial_r = \frac{\partial}{\partial r}$ . For the viscous fluid the Rayleigh criterion (1.1) modifies as follows [18]

$$\text{Ro} + 1 + \frac{1}{4\text{Re}^2} < 0 \quad (1.3)$$

and reduces to the diffusionless criterion (1.1) as the Reynolds number,  $\text{Re} \rightarrow \infty$ .

In the general multiple-diffusive case the existence of such a direct correspondence between the diffusionless and diffusive stability criteria is not evident. In many cases, however, the reduction of the double-diffusive instability criteria to the diffusionless ones can be achieved by setting the corresponding Prandtl number to 1 and then tending diffusivities to zero (or, equivalently, the corresponding Reynolds numbers to infinity).

Indeed, the stationary axisymmetric instability known as the double-diffusive Goldreich-Schubert-Fricke (GSF) instability [1, 40] develops in the rotating viscous and thermally conducting fluid when the extended Rayleigh criterion is fulfilled

$$4(\text{Ro} + 1) + \text{Pr} \frac{N^2}{\Omega^2} + \frac{1}{\text{Re}^2} < 0, \quad (1.4)$$

where  $N$  is the Brunt-Väisälä frequency<sup>1</sup> [6]

$$N^2 := \frac{g}{\gamma} \frac{\partial}{\partial r} \ln(p\rho^{-\gamma}) = \frac{g}{\gamma} \left( \frac{1}{p} \frac{\partial p}{\partial r} - \frac{\gamma}{\rho} \frac{\partial \rho}{\partial r} \right),$$

and  $p$  is the pressure of the fluid,  $\rho$  the density,  $\gamma$  the adiabatic index, and  $g$  the radial acceleration. When the dissipative effects are absent,  $\nu = 0$ ,  $\kappa = 0$ , the diffusionless GSF instability occurs for [1]

$$4(\text{Ro} + 1) + \frac{N^2}{\Omega^2} < 0. \quad (1.5)$$

Evidently,  $\text{Pr} = 1$  is the only value at which the criterion (1.4) reduces to (1.5) in the limit  $\text{Re} \rightarrow \infty$ .

Similarly, the Michael's criterion of ideal MHD [42] predicts stationary axisymmetric instability caused by an azimuthal magnetic field for a rotating flow of a non-viscous incompressible Newtonian fluid that is a perfect electrical conductor, if

$$\text{Ro} + 1 - \frac{\omega_{A_\phi}^2}{\Omega^2} \text{Rb} < 0, \quad (1.6)$$

where  $\text{Rb}$  is the magnetic Rossby number [27]

$$\text{Rb} := \frac{r \partial_r \omega_{A_\phi}}{2\omega_{A_\phi}} \quad (1.7)$$

and  $\omega_{A_\phi}$  is the Alfvén angular velocity related to the magnitude of the magnetic field [46]. Again, the diffusionless Michael's criterion (1.6) follows in the limit of  $\text{Re} \rightarrow \infty$  from its double-diffusive counterpart [30]

$$\text{Ro} + 1 - \text{Pm} \frac{\omega_{A_\phi}^2}{\Omega^2} \text{Rb} + \frac{1}{4\text{Re}^2} < 0 \quad (1.8)$$

---

<sup>1</sup> which in the limit of  $\gamma \rightarrow \infty$  reduces to the buoyancy frequency in the Boussinesq approximation  $N^2 = -\frac{g}{\rho} \frac{d\rho}{dr}$ .

only if  $\text{Pm} = 1$ .

Both the diffusionless and the double-diffusive Michael's criteria predict stability with respect to axisymmetric perturbations for the rotating flow and the azimuthal magnetic field that satisfy the following constraints

$$\Omega = \omega_{A\phi}, \quad \text{Ro} = \text{Rb} = -1. \quad (1.9)$$

In 1956 Chandrasekhar [14] observed that the properties (1.9) correspond to an exact steady solution of the MHD equations for an incompressible fluid in the ideal case, i.e. when  $\nu = 0$  and  $\eta = 0$ . On this solution the total pressure of the fluid and the magnetic field is constant, the fluid velocity at every point is parallel to the direction of the magnetic field at that point, and the Alfvén angular velocity is equal to the angular velocity of the fluid, which implies equality of the densities of the fluid magnetic and kinetic energies. This *energy equipartition solution* of the ideal MHD was proven by Chandrasekhar [14] to be marginally stable against *general* perturbations.<sup>2</sup>

Indeed, it was found in [1, 4, 46] that in the limit of infinitely large axial and azimuthal wavenumbers of a non-axisymmetric perturbation, the hydrodynamically stable rotating flow of inviscid and perfectly conducting fluid is destabilized by an azimuthal magnetic field, if

$$\frac{\omega_{A\phi}^2}{\Omega^2} < -\frac{4\text{Ro}}{m^2}, \quad (1.10)$$

where  $m \gg 1$  is the azimuthal wavenumber and  $\text{Ro} < 0$ . Nevertheless, the equipartition solution (1.9) violates the instability condition (1.10) already at  $m > 2$ , which agrees with the Chandrasekhar's theorem [14].

Recently, Bogoyavlenskij [10] discovered that viscous and resistive incompressible MHD equations possess exact *unsteady* equipartition solutions with finite and equal kinetic and magnetic energies when the fluid velocity and the magnetic field are collinear and the kinematic viscosity  $\nu$  is equal to the magnetic diffusivity  $\eta$ , i.e. when  $\text{Pm} = 1$ . Under the constraint  $\text{Pm} = 1$  the Bogoyavlenskij unsteady equipartition solutions turn into the ideal and *steady* Chandrasekhar equipartition equilibria when  $\nu = \eta = 0$  [10].

Summarizing, one could expect that in the double-diffusive MHD the remarkable stability of the Chandrasekhar energy equipartition solution is preserved under the constraint  $\text{Pm} = 1$ . As soon as the constraint is violated, one could anticipate a dissipation-induced instability of the equipartition solution. For instance, recent analytical works [27, 30] demonstrated that in the inductionless limit<sup>3</sup> of  $\text{Pm} = 0$  a rotating viscous incompressible fluid with vanishing electrical conductivity is destabilized by azimuthal magnetic fields of arbitrary radial dependency, if

$$8(\text{Ro} + 1)\text{Rb} > -(\text{Ro} + 2)^2. \quad (1.11)$$

---

<sup>2</sup>A bit surprisingly, as he admitted in his memoirs [15]: “One nice result which nevertheless came out at this time was the proof of the stability of the equipartition solution. Wentzel and Goldberger checked my analysis as I could not quite believe the result myself.” Actually, the Chandrasekhar equipartition solution belongs to a wide class of exact stationary solutions of MHD equations for the case of ideal incompressible infinitely conducting fluid with the constant total pressure that includes even flows with knotted magnetic surfaces [21].

<sup>3</sup>A very small ratio of viscosity of the fluid to its electrical resistivity, typically of order  $10^{-6} - 10^{-5}$ , is a characteristic of liquid metals that are used in laboratory experiments with the magnetized Couette-Taylor flow [49]. In astrophysics and geophysics such small values of  $\text{Pm}$  are typical for the planets interiors, cold parts of accretion disks, and “dead-zones” of the protoplanetary disks [6, 23, 27, 30, 17, 48, 12, 5].

The criterion (1.11) implies destabilization of the Chandrasekhar equipartition solution, which susceptibility to the double-diffusive AMRI at  $\text{Pm} \ll 1$  has been confirmed numerically in [17, 48], as well as instability of the Keplerian rotating flow with  $\text{Ro} = -3/4$  when  $\text{Rb} > -25/32$ .

Since the double-diffusive AMRI is an oscillatory non-axisymmetric instability, its onset is characterized by the classical Hopf bifurcation when simple eigenvalues cross the imaginary axis in the complex plane. On the other hand, the equations of the diffusionless MHD can be written in the Hamiltonian form [45]. By this reason, the stable oscillatory non-axisymmetric modes in the ideal MHD case can carry both positive and negative energy; their interaction yields the Hamilton-Hopf bifurcation at the onset of the non-axisymmetric oscillatory instabilities [43].

In the present work we investigate the singular limit of the onset of the Hopf bifurcation at the threshold of the oscillatory AMRI of a differentially rotating flow of a viscous and electrically conducting fluid in an azimuthal magnetic field of arbitrary radial dependency at arbitrary  $\text{Pm}$ . We show that the threshold of the double-diffusive AMRI tends to the threshold of the diffusionless AMRI only at  $\text{Pm} = 1$  as the Reynolds numbers tend to infinity and find the Whitney umbrella singularity on the neutral stability surface that dictates this specific choice of  $\text{Pm}$ . We re-derive the WKB equations of the system and write the corresponding algebraic eigenvalue problem, which determines the dispersion relation of the ideal system, in the Hamiltonian form. This allows us to study systematically its non-Hamiltonian perturbation by the viscous and resistive terms. We classify the stable oscillatory modes involved in the Hamilton-Hopf bifurcation by their symplectic signature (or energy sign). Then, we explicitly demonstrate by means of the perturbation theory for eigenvalues that when viscosity and ohmic diffusivity are weak (and even infinitesimally small), the domination of viscosity destroys stability of the negative energy mode at  $\text{Pm} > 1$  whereas the domination of ohmic diffusivity destabilizes the positive energy mode at  $\text{Pm} < 1$  (including the inductionless case  $\text{Pm} = 0$ ) in the close vicinity of the Hamilton-Hopf bifurcation. However, when the fluid Rossby number exceeds some critical value, the destabilization is possible only at finite values of Reynolds numbers and is accompanied by a transfer of instability between negative- and positive-energy modes that happens due to presence of complex exceptional points in the spectrum.

Using these results we find the conditions for the azimuthal MRI to be a dissipation-induced instability of the Chandrasekhar equipartition solution and its extensions. We obtain a unifying geometric picture that naturally connects the diffusionless and double-diffusive AMRI in low- and high- $\text{Pm}$  regimes in the spirit of the singularity theory approach by Bottema [11] and Arnold [3] on generic singularities in the multiparameter families of matrices, which is especially efficient when combined with the perturbation of multiple eigenvalues, index theory and exploitation of the fundamental symmetries of the ideal system [38, 39, 13, 28, 29].

## 2 Transport equation for amplitudes and its dispersion relation

### 2.1 Governing equations and the background fields

Dynamics of a flow of a viscous and electrically conducting incompressible fluid that interacts with the magnetic field is described by the Navier-Stokes equation for the fluid velocity  $\mathbf{u}$  which is coupled with the induction equation for the magnetic field  $\mathbf{B}$  [6, 30]

$$\begin{aligned}\frac{\partial \mathbf{u}}{\partial t} + \mathbf{u} \cdot \nabla \mathbf{u} - \frac{1}{\mu_0 \rho} \mathbf{B} \cdot \nabla \mathbf{B} + \frac{1}{\rho} \nabla P - \nu \nabla^2 \mathbf{u} &= 0, \\ \frac{\partial \mathbf{B}}{\partial t} + \mathbf{u} \cdot \nabla \mathbf{B} - \mathbf{B} \cdot \nabla \mathbf{u} - \eta \nabla^2 \mathbf{B} &= 0.\end{aligned}\quad (2.1)$$

In the equations (2.1) the total pressure is denoted by  $P = p + \frac{\mathbf{B}^2}{2\mu_0}$ ,  $p$  is the hydrodynamic pressure,  $\rho = \text{const}$  the density,  $\nu = \text{const}$  the kinematic viscosity,  $\eta = (\mu_0 \sigma)^{-1}$  the magnetic diffusivity,  $\sigma = \text{const}$  the conductivity of the fluid, and  $\mu_0$  the magnetic permeability of free space. In addition, the incompressible flow and the solenoidal magnetic field fulfil the constraints:

$$\nabla \cdot \mathbf{u} = 0, \quad \nabla \cdot \mathbf{B} = 0. \quad (2.2)$$

Let in the steady-state the background flow be differentially rotating in a gap between the radii  $r_1$  and  $r_2 > r_1$  with the angular velocity profile  $\Omega(r)$  that depends only on the radial coordinate  $r$  in the cylindrical coordinate system  $(r, \phi, z)$ . Let the background magnetic field have only an azimuthal component  $B_\phi^0(r)$ , and let the hydrodynamic pressure depend only on  $r$ :

$$\mathbf{u}_0(r) = r \Omega(r) \mathbf{e}_\phi, \quad p = p_0(r), \quad \mathbf{B}_0(r) = B_\phi^0(r) \mathbf{e}_\phi. \quad (2.3)$$

In 1956 Chandrasekhar [14] observed that, particularly,  $\Omega = \frac{B_\phi^0}{r\sqrt{\rho\mu_0}}$  and  $P = \text{const}$  represent an exact stationary solution of the equations (2.1) and (2.2) in the ideal case, i.e. when  $\nu = 0$  and  $\eta = 0$ . On this solution the kinetic and magnetic energies are in equipartition,  $\frac{\rho(\Omega r)^2}{2} = \frac{(B_\phi^0)^2}{2\mu_0}$ , and  $\text{Ro} = \text{Rb} = -1$ . The latter equality follows from the condition of the constant total pressure and from the fact that in the steady-state the centrifugal acceleration of the background flow is compensated by the pressure gradient,  $r\Omega^2 = \frac{1}{\rho} \partial_r p_0$  [30]. Note that  $\text{Ro} = -1$  corresponds to the velocity profile  $\Omega(r) \sim r^{-2}$  whereas  $\text{Rb} = -1$  corresponds to the magnetic field produced by an axial current  $I$  isolated from the fluid [30, 49]:  $B_\phi^0(r) = \frac{\mu_0 I}{2\pi r}$ .

Linearizing equations (2.1)-(2.2) in the vicinity of the stationary solution (2.3) by assuming general perturbations  $\mathbf{u} = \mathbf{u}_0 + \mathbf{u}'$ ,  $p = p_0 + p'$ , and  $\mathbf{B} = \mathbf{B}_0 + \mathbf{B}'$ , leaving only the terms of first order with respect to the primed quantities, and introducing the gradients of the background fields represented by the two  $3 \times 3$  matrices

$$\mathcal{U} := \nabla \mathbf{u}_0 = \Omega \begin{pmatrix} 0 & -1 & 0 \\ 1 + 2\text{Ro} & 0 & 0 \\ 0 & 0 & 0 \end{pmatrix}, \quad \mathcal{B} := \nabla \mathbf{B}_0 = \frac{B_\phi^0}{r} \begin{pmatrix} 0 & -1 & 0 \\ 1 + 2\text{Rb} & 0 & 0 \\ 0 & 0 & 0 \end{pmatrix}, \quad (2.4)$$

we arrive at the linearized system of magnetohydrodynamics [30, 32, 27]

$$\begin{pmatrix} \partial_t + \mathcal{U} + \mathbf{u}_0 \cdot \nabla - \nu \nabla^2 & -\frac{\mathcal{B} + \mathbf{B}_0 \cdot \nabla}{\rho \mu_0} \\ \mathcal{B} - \mathbf{B}_0 \cdot \nabla & \partial_t - \mathcal{U} + \mathbf{u}_0 \cdot \nabla - \eta \nabla^2 \end{pmatrix} \begin{pmatrix} \mathbf{u}' \\ \mathbf{B}' \end{pmatrix} = -\frac{\nabla}{\rho} \begin{pmatrix} p' + \frac{\mathbf{B}_0 \cdot \mathbf{B}'}{\mu_0} \\ 0 \end{pmatrix}, \quad (2.5)$$

where the perturbations fulfil the constraints

$$\nabla \cdot \mathbf{u}' = 0, \quad \nabla \cdot \mathbf{B}' = 0. \quad (2.6)$$

## 2.2 Derivation of the amplitude transport equations

Following [2, 18], we assume that  $\nu = \epsilon^2 \tilde{\nu}$  and  $\eta = \epsilon^2 \tilde{\eta}$  and seek for solutions of the linearized equations (2.5) in the form of the generalized progressive wave expansions with respect to the small parameter  $\epsilon$ ,  $0 < \epsilon \ll 1$  [19]:

$$\mathbf{A}'(\mathbf{x}, t, \epsilon) = e^{i\Phi(\mathbf{x}, t)/\epsilon} \left( \mathbf{A}^{(0)}(\mathbf{x}, t) + \epsilon \mathbf{A}^{(1)}(\mathbf{x}, t) \right) + \epsilon \mathbf{A}^{(r)}(\mathbf{x}, t, \epsilon), \quad (2.7)$$

where  $\mathbf{A}' = (\mathbf{u}', \mathbf{B}', p')^T$ ,  $\mathbf{A}^{(j)} = (\mathbf{u}^{(j)}, \mathbf{B}^{(j)}, p^{(j)})^T$ ,  $\mathbf{x}$  is a vector of coordinates,  $\Phi$  represents the phase of the wave or the eikonal, and  $\mathbf{u}^{(j)}$ ,  $\mathbf{B}^{(j)}$ , and  $p^{(j)}$ ,  $j = 0, 1, r$ , are complex-valued amplitudes. The index  $r$  denotes the remainder terms that are assumed to be uniformly bounded in  $\epsilon$  on any fixed time interval [35, 36].

Substituting expansions (2.7) in (2.5) and collecting terms at  $\epsilon^{-1}$  and  $\epsilon^0$ , we find [30]

$$\begin{aligned} \epsilon^{-1} : & \begin{pmatrix} \partial_t \Phi + (\mathbf{u}_0 \cdot \nabla \Phi) & -\frac{(\mathbf{B}_0 \cdot \nabla \Phi)}{\rho \mu_0} \\ -(\mathbf{B}_0 \cdot \nabla \Phi) & \partial_t \Phi + (\mathbf{u}_0 \cdot \nabla \Phi) \end{pmatrix} \begin{pmatrix} \mathbf{u}^{(0)} \\ \mathbf{B}^{(0)} \end{pmatrix} = -\frac{\nabla \Phi}{\rho} \begin{pmatrix} p^{(0)} + \frac{\mathbf{B}_0 \cdot \mathbf{B}^{(0)}}{\mu_0} \\ 0 \end{pmatrix} \quad (2.8) \\ \epsilon^0 : & i \begin{pmatrix} \partial_t \Phi + (\mathbf{u}_0 \cdot \nabla \Phi) & -\frac{(\mathbf{B}_0 \cdot \nabla \Phi)}{\rho \mu_0} \\ -(\mathbf{B}_0 \cdot \nabla \Phi) & \partial_t \Phi + (\mathbf{u}_0 \cdot \nabla \Phi) \end{pmatrix} \begin{pmatrix} \mathbf{u}^{(1)} \\ \mathbf{B}^{(1)} \end{pmatrix} + i \frac{\nabla \Phi}{\rho} \begin{pmatrix} p^{(1)} + \frac{\mathbf{B}_0 \cdot \mathbf{B}^{(1)}}{\mu_0} \\ 0 \end{pmatrix} \\ & + \begin{pmatrix} \partial_t + \mathcal{U} + \mathbf{u}_0 \cdot \nabla + \tilde{\nu}(\nabla \Phi)^2 & -\frac{\mathcal{B} + \mathbf{B}_0 \cdot \nabla}{\rho \mu_0} \\ \mathcal{B} - \mathbf{B}_0 \cdot \nabla & \partial_t - \mathcal{U} + \mathbf{u}_0 \cdot \nabla + \tilde{\eta}(\nabla \Phi)^2 \end{pmatrix} \begin{pmatrix} \mathbf{u}^{(0)} \\ \mathbf{B}^{(0)} \end{pmatrix} \\ & + \frac{\nabla}{\rho} \begin{pmatrix} p^{(0)} + \frac{\mathbf{B}_0 \cdot \mathbf{B}^{(0)}}{\mu_0} \\ 0 \end{pmatrix} = 0. \quad (2.9) \end{aligned}$$

The solenoidality conditions (2.6) yield

$$\begin{aligned} \mathbf{u}^{(0)} \cdot \nabla \Phi &= 0, & \nabla \cdot \mathbf{u}^{(0)} + i \mathbf{u}^{(1)} \cdot \nabla \Phi &= 0, \\ \mathbf{B}^{(0)} \cdot \nabla \Phi &= 0, & \nabla \cdot \mathbf{B}^{(0)} + i \mathbf{B}^{(1)} \cdot \nabla \Phi &= 0. \end{aligned} \quad (2.10)$$

Taking the dot product of the first of the equations in the system (2.8) with  $\nabla \Phi$  under the constraints (2.10) we find that for  $\nabla \Phi \neq 0$

$$p^{(0)} = -\frac{\mathbf{B}_0 \cdot \mathbf{B}^{(0)}}{\mu_0}. \quad (2.11)$$



Under the condition (2.11) the equation (2.8) has a nontrivial solution if the determinant of the  $6 \times 6$  matrix in its left-hand side is vanishing. This gives us two characteristic roots corresponding to the two Alfvén waves [32, 19] that originate the following two Hamilton-Jacobi equations:

$$\partial_t \Phi + \left( \mathbf{u}_0 \pm \frac{\mathbf{B}_0}{\sqrt{\rho\mu_0}} \right) \cdot \nabla \Phi = 0. \quad (2.12)$$

The characteristic roots  $\left( -\mathbf{u}_0 \pm \frac{\mathbf{B}_0}{\sqrt{\rho\mu_0}} \right) \cdot \nabla \Phi$  are triple and semi-simple that degenerate into a semi-simple characteristic root of multiplicity 6 on the surface [32, 19]

$$\mathbf{B}_0 \cdot \nabla \Phi = 0. \quad (2.13)$$

When (2.13) is fulfilled, the derivative of the phase along the fluid stream lines vanishes:

$$\frac{D\Phi}{Dt} := \partial_t \Phi + \mathbf{u}_0 \cdot \nabla \Phi = 0. \quad (2.14)$$

With the use of the relations (2.11), (2.13), (2.14) we simplify the equations (2.9):

$$\begin{aligned} \left( \frac{D}{Dt} + \tilde{\nu}(\nabla \Phi)^2 + \mathcal{U} \right) \mathbf{u}^{(0)} - \frac{1}{\rho\mu_0} (\mathcal{B} + \mathbf{B}_0 \cdot \nabla) \mathbf{B}^{(0)} &= -\frac{i}{\rho} \left( p^{(1)} + \frac{1}{\mu_0} (\mathbf{B}_0 \cdot \mathbf{B}^{(1)}) \right) \nabla \Phi, \\ \left( \frac{D}{Dt} + \tilde{\eta}(\nabla \Phi)^2 - \mathcal{U} \right) \mathbf{B}^{(0)} + (\mathcal{B} - \mathbf{B}_0 \cdot \nabla) \mathbf{u}^{(0)} &= 0. \end{aligned} \quad (2.15)$$

Eliminating pressure in the first of Eqs. (2.15) via multiplication of it by  $\nabla \Phi$  and taking into account the constraints (2.10), then using the identities

$$\begin{aligned} \nabla \partial_t \Phi + \nabla(\mathbf{u}_0 \cdot \nabla) \Phi &= \frac{D}{Dt} \nabla \Phi + \mathcal{U}^T \nabla \Phi = 0, \\ \nabla(\mathbf{B}_0 \cdot \nabla \Phi) &= (\mathbf{B}_0 \cdot \nabla) \nabla \Phi + \mathcal{B}^T \nabla \Phi = 0, \\ \frac{D}{Dt} (\nabla \Phi \cdot \mathbf{u}^{(0)}) &= \frac{D \nabla \Phi}{Dt} \cdot \mathbf{u}^{(0)} + \nabla \Phi \cdot \frac{D \mathbf{u}^{(0)}}{Dt} = 0, \\ (\mathbf{B}_0 \cdot \nabla) (\nabla \Phi \cdot \mathbf{B}^{(0)}) &= ((\mathbf{B}_0 \cdot \nabla) \nabla \Phi) \cdot \mathbf{B}^{(0)} + \nabla \Phi \cdot (\mathbf{B}_0 \cdot \nabla) \mathbf{B}^{(0)} = 0, \end{aligned} \quad (2.16)$$

and, finally, denoting  $\mathbf{k} = \nabla \Phi$ , we write the transport equations for the amplitudes (2.15) as

$$\begin{aligned} \frac{D \mathbf{u}^{(0)}}{Dt} &= - \left( \mathcal{I} - \frac{2\mathbf{k}\mathbf{k}^T}{|\mathbf{k}|^2} \right) \mathcal{U} \mathbf{u}^{(0)} - \tilde{\nu} |\mathbf{k}|^2 \mathbf{u}^{(0)} + \frac{1}{\rho\mu_0} \left( \left( \mathcal{I} - \frac{2\mathbf{k}\mathbf{k}^T}{|\mathbf{k}|^2} \right) \mathcal{B} + \mathbf{B}_0 \cdot \nabla \right) \mathbf{B}^{(0)}, \\ \frac{D \mathbf{B}^{(0)}}{Dt} &= \mathcal{U} \mathbf{B}^{(0)} - \tilde{\eta} |\mathbf{k}|^2 \mathbf{B}^{(0)} - (\mathcal{B} - \mathbf{B}_0 \cdot \nabla) \mathbf{u}^{(0)}, \end{aligned} \quad (2.17)$$

where  $\mathcal{I}$  is a  $3 \times 3$  identity matrix. From the phase equation (2.16) we deduce that

$$\frac{D \mathbf{k}}{Dt} = -\mathcal{U}^T \mathbf{k}. \quad (2.18)$$

The equations (2.18) and (2.17) are valid under the assumption that the condition (2.13) is fulfilled.

The local partial differential equations (2.17) are fully equivalent to the transport equations of [29, 30]. In the case of the ideal MHD when viscosity and resistivity are zero, the equations (2.17) exactly coincide with those of the work [32] and are fully equivalent to the



transport equations derived in [20]. In the absence of the magnetic field these equations are reduced to that of the work [18] that considered stability of the viscous Couette-Taylor flow.

Note that the leading order terms dominate the solution (2.7) for a sufficiently long time, provided that  $\epsilon$  is small enough [35, 36], which reduces analysis of instabilities to the investigation of the growth rates of solutions of the transport equations (2.17).

According to [18] and [20], in order to study physically relevant and potentially unstable modes we have to choose bounded and asymptotically non-decaying solutions of the system (2.18). These correspond to  $k_\phi \equiv 0$  and  $k_R$  and  $k_z$  time-independent. Note that this solution is compatible with the constraint  $\mathbf{B}_0 \cdot \mathbf{k} = 0$  following from (2.13).

### 2.3 Dispersion relation of the double-diffusive amplitude equations

Denote  $\alpha = k_z |\mathbf{k}|^{-1}$ ,  $|\mathbf{k}|^2 = k_R^2 + k_z^2$  and introduce the Alfvén angular velocity, the viscous and resistive frequencies, and the hydrodynamic and magnetic Reynolds numbers [30]:

$$\omega_{A_\phi} = \frac{B_\phi^0}{R\sqrt{\rho\mu_0}}, \quad \omega_\nu = \tilde{\nu}|\mathbf{k}|^2, \quad \omega_\eta = \tilde{\eta}|\mathbf{k}|^2, \quad \text{Re} = \frac{\alpha\Omega}{\omega_\nu}, \quad \text{Rm} = \frac{\alpha\Omega}{\omega_\eta}. \quad (2.19)$$

In particular,  $\text{Rm} = \text{RePm}$ .

Looking for a solution to Eqs. (2.17) in the modal form [20]:  $\mathbf{u}^{(0)} = \hat{\mathbf{u}}e^{\alpha\Omega\lambda t + im\phi}$ ,  $\mathbf{B}^{(0)} = \sqrt{\rho\mu_0}\hat{\mathbf{B}}e^{\alpha\Omega\lambda t + im\phi}$  we write the amplitude equations in the matrix form

$$\mathbf{A}\mathbf{z} = \lambda\mathbf{z}, \quad (2.20)$$

where  $\mathbf{z} = (\hat{u}_R, \hat{u}_\phi, \hat{B}_R, \hat{B}_\phi)^T \in \mathbb{C}^4$  and  $\mathbf{A} = \mathbf{A}_0 + \mathbf{A}_1 \in \mathbb{C}^{4 \times 4}$  with [30, 27, 53]

$$\mathbf{A}_0 = \begin{pmatrix} -in & 2\alpha & inS & -2\alpha S \\ -\frac{2(1+\text{Ro})}{\alpha} & -in & \frac{2(1+\text{Rb})}{\alpha}S & inS \\ inS & 0 & -in & 0 \\ -\frac{2\text{Rb}}{\alpha}S & inS & \frac{2\text{Ro}}{\alpha} & -in \end{pmatrix}, \quad \mathbf{A}_1 = \begin{pmatrix} \frac{-1}{\text{Re}} & 0 & 0 & 0 \\ 0 & \frac{-1}{\text{Re}} & 0 & 0 \\ 0 & 0 & \frac{-1}{\text{Rm}} & 0 \\ 0 & 0 & 0 & \frac{-1}{\text{Rm}} \end{pmatrix}. \quad (2.21)$$

The ratio  $n = \frac{m}{\alpha}$  is the modified azimuthal wavenumber and  $S = \frac{\omega_{A_\phi}}{\Omega}$  is the Alfvén angular velocity in the units of  $\Omega$ .

Let us introduce a Hermitian matrix

$$\mathbf{G} = \begin{pmatrix} 0 & -i & 0 & iS \\ i & 0 & -iS & 0 \\ 0 & iS & 4\frac{\text{Ro}-\text{Rb}}{\alpha n} & -i \\ -iS & 0 & i & 0 \end{pmatrix} \quad (2.22)$$

and define an indefinite inner product in  $\mathbb{C}^4$  as  $[\mathbf{x}, \mathbf{y}] = \bar{\mathbf{y}}^T \mathbf{G} \mathbf{x}$  [58, 29] and a standard inner product as  $(\mathbf{x}, \mathbf{y}) = \bar{\mathbf{y}}^T \mathbf{x}$ . The matrix  $\mathbf{H}_0 = -i\mathbf{G}\mathbf{A}_0$  is Hermitian too:

$$\mathbf{H}_0 = \begin{pmatrix} -\frac{2(S^2\text{Rb}-\text{Ro}-1)}{\alpha} & in(S^2+1) & -\frac{2S(1+\text{Rb}-\text{Ro})}{\alpha} & -2inS \\ -in(S^2+1) & 2\alpha & 2inS & -2\alpha S \\ -\frac{2S(1+\text{Rb}-\text{Ro})}{\alpha} & -2inS & \frac{2(S^2\text{Rb}+S^2+2\text{Rb}-3\text{Ro})}{\alpha} & in(S^2+1) \\ 2inS & -2\alpha S & -in(S^2+1) & 2\alpha S^2 \end{pmatrix}. \quad (2.23)$$

Consequently, the eigenvalue problem  $\mathbf{A}_0 \mathbf{z} = \lambda \mathbf{z}$  can be written in the Hamiltonian form with the Hamiltonian  $\mathbf{H}_0$  [58, 29]:

$$\mathbf{H}_0 \mathbf{z} = i^{-1} \mathbf{G} \lambda \mathbf{z}. \quad (2.24)$$

The fundamental symmetry

$$\mathbf{A}_0 = -\mathbf{G}^{-1} \overline{\mathbf{A}_0}^T \mathbf{G}, \quad (2.25)$$

where the overbar denotes complex conjugation, implies the symmetry of the spectrum of the matrix  $\mathbf{A}_0$  with respect to the imaginary axis [58, 29].

The full eigenvalue problem (2.20) is thus a dissipative perturbation of the Hamiltonian eigenvalue problem (2.24)

$$(\mathbf{H}_0 + \mathbf{H}_1) \mathbf{z} = i^{-1} \mathbf{G} \lambda \mathbf{z}, \quad (2.26)$$

where  $\mathbf{H}_1 = -i \mathbf{G} \mathbf{A}_1$  is a complex non-Hermitian matrix:

$$\mathbf{H}_1 = \begin{pmatrix} 0 & \frac{1}{\text{Re}} & 0 & -\frac{S}{\text{Rm}} \\ -\frac{1}{\text{Re}} & 0 & \frac{S}{\text{Rm}} & 0 \\ 0 & -\frac{S}{\text{Re}} & 4i \frac{\text{Ro}-\text{Rb}}{\alpha n \text{Rm}} & \frac{1}{\text{Rm}} \\ \frac{S}{\text{Re}} & 0 & -\frac{1}{\text{Rm}} & 0 \end{pmatrix}. \quad (2.27)$$

The complex characteristic equation  $p(\lambda) := \det(\mathbf{H}_0 + \mathbf{H}_1 - i^{-1} \mathbf{G} \lambda \mathbf{I}) = 0$ , where  $\mathbf{I}$  is the  $4 \times 4$  identity matrix, is the dispersion relation for the double-diffusive system (2.26).

### 3 Linear Hamilton-Hopf bifurcation and the diffusionless AMRI

#### 3.1 Neutral stability curves

Let  $\delta := \text{Ro} - \text{Rb} S^2$ . In the Hamiltonian case ( $\frac{1}{\text{Re}} = 0$ ,  $\frac{1}{\text{Rm}} = 0$ ) the dispersion relation  $p_0(\lambda) := \det(\mathbf{H}_0 - i^{-1} \mathbf{G} \lambda \mathbf{I}) = 0$  possesses a compact representation [20, 46, 30]

$$p_0(\lambda) = 4\delta^2 + 4(i\lambda - n + nS^2)^2 - (2\delta - (i\lambda - n)^2 + n^2 S^2)^2 = 0. \quad (3.1)$$

If  $\delta = 0$ , i.e.  $\text{Ro} = \text{Rb} S^2$ , then the equation (3.1) simplifies and its roots are [30]

$$\begin{aligned} \lambda_{1,2} &= -i(1+n) \pm i\sqrt{1 - S^2[1 - (1+n)^2]}, \\ \lambda_{3,4} &= -i(1-n) \pm i\sqrt{1 - S^2[1 - (1-n)^2]}. \end{aligned} \quad (3.2)$$

The eigenvalues  $\lambda_{1,2,3,4}$  are imaginary and simple for all  $0 < n \leq 2$ , if  $0 \leq S < 1$ . The equality  $S = 1$  implies  $\text{Ro} = \text{Rb}$  and the existence of the double zero eigenvalue which is semi-simple at all  $0 \leq n \leq 2$  but  $n = 1$  where it has a Jordan block of order 2; the other two eigenvalue branches are formed by simple imaginary eigenvalues (marginal stability). At  $S > 1$  complex eigenvalues originate (oscillatory instability), if

$$S > \frac{1}{\sqrt{1 - (1-n)^2}}. \quad (3.3)$$

At the boundary of the domain (3.3) the eigenvalues are double imaginary with the Jordan block.

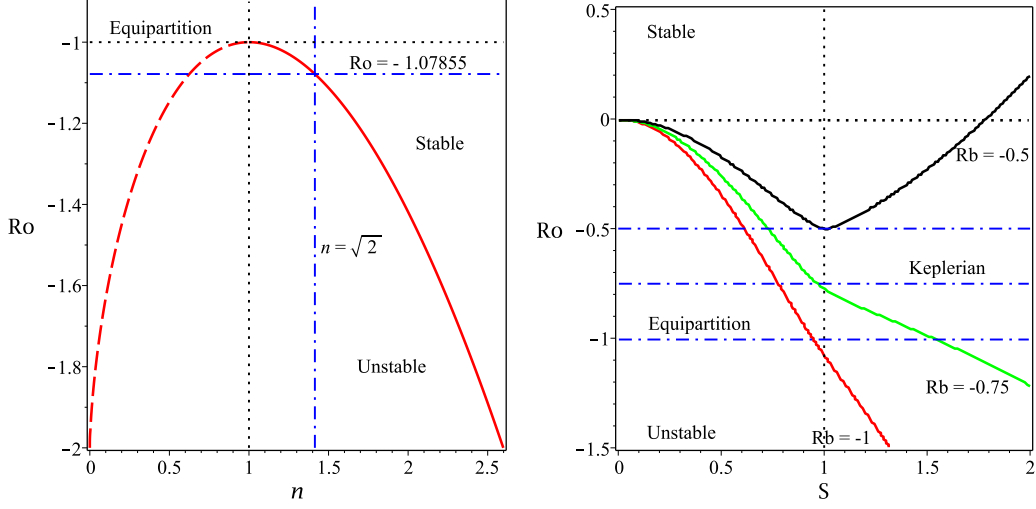


Figure 1: (Left) Stability diagram in  $(n, \text{Ro})$ -plane at  $S = 1$  and  $\text{Rb} = -1$  according to the criterion (3.5). The dashed line shows the nonphysical branch of the neutral stability curve (3.7) corresponding to  $0 < n < 1$ . (Right) The critical value of  $\text{Ro}$  at the onset of the Hamilton-Hopf bifurcation as a function of  $S$  when  $n = \sqrt{-2\text{Rb}}$  [30] at various values of  $\text{Rb}$ .

In general, the instability corresponds to the negative discriminant of the polynomial (3.1):

$$\begin{aligned} & (nS)^6(S^2 - 1)^2 + 2(nS)^4[(S^2 + 1)\delta^2 + 2(S^2 - 1)(S^2 - 2)\delta + (S^2 - 1)^2(1 - 2S^2)] \\ & + (nS)^2[\delta^4 + 4(2S^2 + 3)\delta^3 - 2(4S^4 + 11(S^2 - 1))\delta^2 + 4(S^2 - 1)(5S^2 - 3)\delta + (S^2 - 1)^2] \\ & - 4\delta(\delta + 1)^3(S^2 - \delta - 1) < 0. \end{aligned} \quad (3.4)$$

Following [46] we assume in (3.4) that  $nS = c$ , where  $c = \text{const}$ . Taking into account that  $\delta = \text{Ro} - \text{Rb}S^2$  and then taking the limit  $S \rightarrow 0$ , which obviously corresponds to the limit of  $n \rightarrow \infty$ , we find the following asymptotic expression for the instability condition [46]:

$$(c^2 + 4\text{Ro})(\text{Ro} + 1)^2 + c^2 < 0,$$

or  $S^2 < -\frac{4\text{Ro}}{n^2}$ , which yields (1.10) at  $\alpha = 1$ . At  $n = 0$  the inequality (3.4) reduces to  $\delta < -1$  which is exactly the diffusionless Michael's criterion (1.6).

Let us now assume that  $S = 1$ . Then, the inequality (3.4) takes the form

$$4n^4 + ((\text{Ro} - \text{Rb})^2 + 20(\text{Ro} - \text{Rb}) - 8)n^2 + 4(\text{Ro} - \text{Rb} + 1)^3 < 0 \quad (3.5)$$

and the dispersion relation at  $S = 1$  factorizes as follows:

$$p_0(\lambda)|_{S=1} = [\lambda^3 + 4in\lambda^2 + 4(1 - n^2 + \text{Ro} - \text{Rb})\lambda + 8in(\text{Ro} - \text{Rb})]\lambda = 0. \quad (3.6)$$

The equality in the criterion (3.5) corresponds to the transition from marginal stability to oscillatory instability, see Fig. 1. At the marginal stability curve one of the eigenvalues

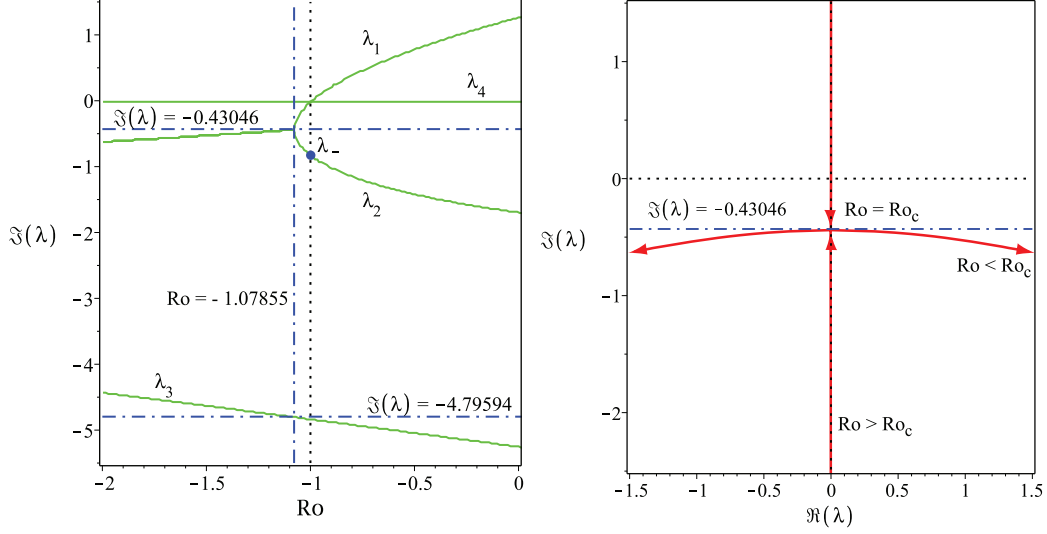


Figure 2: (Left) Frequencies of the roots of the dispersion relation (3.6) when  $Rb = -1$  and  $n = \sqrt{2}$  demonstrating the Hamilton-Hopf bifurcation at  $Ro = Ro_c \approx -1.07855$  and the marginal stability of the Chandrasekhar energy equipartition solution at  $Ro = -1$ . (Right) The linear Hamilton-Hopf bifurcation in the complex plane: with the decrease in  $Ro$  two simple imaginary eigenvalues collide into a double imaginary eigenvalue with the Jordan block (an *exceptional point* [29]) that subsequently splits into two complex eigenvalues (oscillatory instability).

$\lambda$  is always zero and simple, another one is simple and imaginary and the last two form a double and imaginary eigenvalue with the Jordan block. At  $S = 1$  and  $Rb = -1$  the critical value of the fluid Rossby number follows from (3.5) and is equal to

$$Ro_c(n) = -2 + \frac{\beta^{\frac{1}{3}} - n^2}{12} - \frac{n^2}{\beta^{\frac{1}{3}}} \left( 18 - \frac{n^2}{12} \right), \quad (3.7)$$

where

$$\beta(n) = -n^2 \left( n^4 + 540n^2 - 5832 - 24\sqrt{3(n^2 + 27)^3} \right). \quad (3.8)$$

For example, at  $n = \sqrt{2}$  Eq. (3.7) yields  $Ro_c \approx -1.07855$ , corresponding to the intersection of the two dash-dot lines in Fig. 1(left). At this point of the curve (3.7) the eigenvalues are  $\lambda_1 = \lambda_2 = \lambda_c$  (Fig. 2), where

$$\lambda_c = \frac{i\sqrt{2}}{34347} \left\{ \frac{9\sqrt{87} + 136}{4} \left[ \beta(\sqrt{2}) \right]^{\frac{2}{3}} + \frac{321\sqrt{87} - 2782}{2} \left[ \beta(\sqrt{2}) \right]^{\frac{1}{3}} - 57245 \right\} \approx -i0.43046, \quad (3.9)$$

$$\lambda_3 \approx -i4.79594, \quad \lambda_4 = 0.$$

### 3.2 The Krein collision at the linear Hamilton-Hopf bifurcation threshold

At  $Ro = Rb = -1$  and  $S = 1$ , Eq. (3.2) yields a double semi-simple zero eigenvalue  $\lambda_0 = 0$  with the two linearly-independent eigenvectors  $\mathbf{z}_1 = (0, 1, 0, 1)^T$  and  $\mathbf{z}_2 = (1, 0, 1, 0)^T$  and

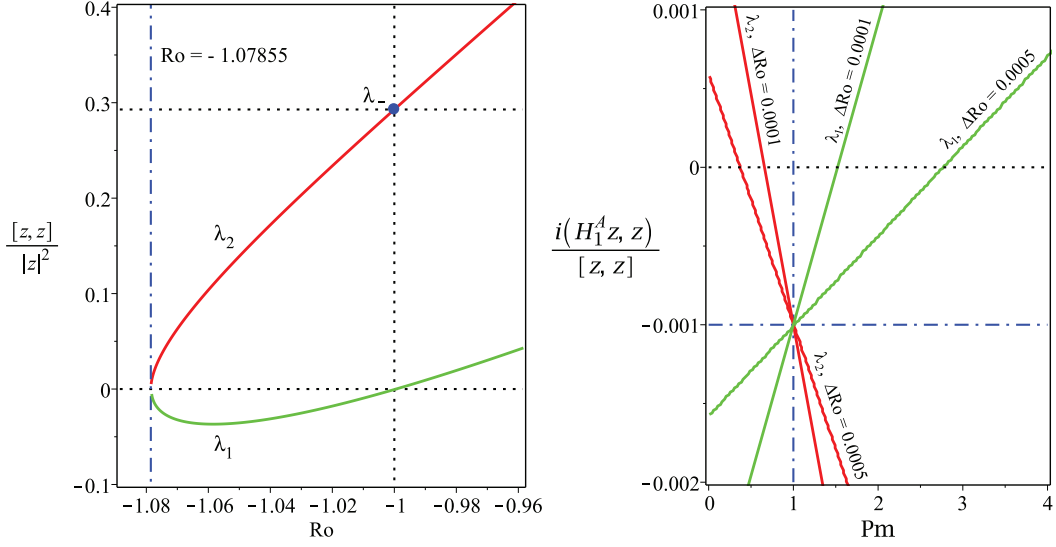


Figure 3: For  $S = 1$ ,  $Rb = -1$ ,  $n = \sqrt{2}$ , and  $\alpha = 1$  (left) the values of the normalized indefinite inner product  $\frac{[z, z]}{|z|^2}$  calculated with the eigenvectors at the imaginary eigenvalues  $\lambda_1$  and  $\lambda_2$  shown in Fig. 2(left) that participate in the Hamilton-Hopf bifurcation at  $Ro = Ro_c \approx -1.07855$ . For  $Ro_c < Ro < -1$  the Krein sign of  $\lambda_1$  is negative and the Krein sign of  $\lambda_2$  is positive. (Right) For  $Rm = 1000$  the values of the real increment  $\delta\lambda^A$  to eigenvalues  $\lambda_1$  with the negative Krein sign and to eigenvalues  $\lambda_2$  with the positive Krein sign according to Eq. (4.1). The interval of negative increments (stability) around  $Pm = 1$  becomes more narrow as  $\Delta Ro := Ro - Ro_c$  tends to zero.

the two imaginary eigenvalues  $\lambda_{\pm} = -2i(n \pm 1)$  with the eigenvectors  $\mathbf{z}_+ = \left(-i\alpha, \frac{-n}{2+n}, \frac{in\alpha}{2+n}, 1\right)^T$  and  $\mathbf{z}_- = \left(i\alpha, \frac{n}{2-n}, \frac{in\alpha}{2-n}, 1\right)^T$ , respectively, where  $n = \sqrt{2}$ , see Fig. 2(left).

It is well-known [58, 13, 29] that imaginary eigenvalues of a Hamiltonian system possess an invariant — the Krein (or symplectic) sign. If  $\lambda = i\omega$  is a simple and imaginary eigenvalue of the eigenvalue problem (2.24), then the Krein sign is the sign of the indefinite scalar product  $[z, z]$ , where  $\mathbf{z}$  is the eigenvector at  $\lambda$ . For instance, the eigenvalues  $\lambda_+$  and  $\lambda_-$  of the Chandrasekhar's equipartition solution have the opposite Krein signs:

$$\frac{[z_+, z_+]}{(z_+, z_+)} = -\frac{2\alpha}{1 + \alpha^2} \frac{2(n+1)^2}{1 + (n+1)^2} < 0, \quad \frac{[z_-, z_-]}{(z_-, z_-)} = \frac{2\alpha}{1 + \alpha^2} \frac{2(n-1)^2}{1 + (n-1)^2} > 0. \quad (3.10)$$

For instance, at  $n = \sqrt{2}$  we have  $\frac{1+\alpha^2}{2\alpha} \frac{[z_-, z_-]}{(z_-, z_-)} = 1 - \frac{\sqrt{2}}{2} \approx 0.2929$ , which means the positive Krein sign of  $\lambda_-$ , see Fig. 3(left). The solid circle corresponding to  $\lambda_-$  in Fig. 3(left) belongs to the curve of the values of the normalized indefinite inner products  $\frac{[z, z]}{|z|^2}$  calculated on the eigenvectors at the eigenvalues of the branch marked as  $\lambda_2$  in Fig. 2(left). All imaginary eigenvalues  $\lambda_2$  for  $Ro_c < Ro < -1$  have positive Krein sign. In contrast, the eigenvalues of the branch  $\lambda_1$  in Fig. 2(left) have negative Krein sign on the same interval.

Therefore, the onset of the nonaxisymmetric oscillatory instability (or the diffusionless AMRI) is accompanied by the Krein collision of the modes of positive and negative Krein

sign, in accordance with the results of [43] who established the interaction of the waves of positive and negative energy at the onset of the diffusionless AMRI. Note that the Krein sign is directly related to the sign of energy of a mode and the linear Hamilton-Hopf bifurcation is a collision of two imaginary eigenvalues of a Hamiltonian system with the opposite Krein (energy) signs [29, 58, 13].

## 4 Dissipation-induced instabilities of the double-diffusive system

### 4.1 Dissipative perturbation of simple imaginary eigenvalues

The complex non-Hermitian matrix of the dissipative perturbation can be decomposed into its Hermitian and anti-Hermitian components:  $\mathbf{H}_1 = \mathbf{H}_1^H + \mathbf{H}_1^A$ , where  $\mathbf{H}_1^H$  is an anti-diagonal matrix  $\mathbf{H}_1^H = \frac{S(Pm-1)}{2Rm} \text{adiag}(1, -1, -1, 1)$  and

$$\mathbf{H}_1^A = \frac{1}{Rm} \begin{pmatrix} 0 & Pm & 0 & -\frac{S(Pm+1)}{2} \\ -Pm & 0 & \frac{S(Pm+1)}{2} & 0 \\ 0 & -\frac{S(Pm+1)}{2} & 4i\frac{Ro-Rb}{\alpha n} & 1 \\ \frac{S(Pm+1)}{2} & 0 & -1 & 0 \end{pmatrix}.$$

At large  $Rm$  an increment  $\delta\lambda$  to a simple imaginary eigenvalue  $\lambda$  with an eigenvector  $\mathbf{z}$  is given by a standard perturbation theory [29, 38, 39, 9] as

$$\delta\lambda = i \frac{\bar{\mathbf{z}}^T \mathbf{H}_1 \mathbf{z}}{\bar{\mathbf{z}}^T \mathbf{G} \mathbf{z}} = i \frac{(\mathbf{H}_1 \mathbf{z}, \mathbf{z})}{[\mathbf{z}, \mathbf{z}]}.$$
 (4.1)

The increment  $\delta\lambda^H = i \frac{(\mathbf{H}_1^H \mathbf{z}, \mathbf{z})}{[\mathbf{z}, \mathbf{z}]}$  is, obviously, imaginary. In general,  $\mathbf{H}_1^H = 0$  at  $Pm = 1$ , i.e. the frequencies are not affected by the Hermitian component of the dissipative perturbation if the contribution from viscosity and resistivity is equal.

In contrast, the increment  $\delta\lambda^A = i \frac{(\mathbf{H}_1^A \mathbf{z}, \mathbf{z})}{[\mathbf{z}, \mathbf{z}]}$  is real. For instance, the eigenvalues  $\lambda_+$  and  $\lambda_-$  of the Chandrasekhar's equipartition solution get the following increments:

$$\delta\lambda_{\pm}^A = -\frac{Pm+1}{2Rm} = -\frac{1}{h} := -\frac{1}{2} \left( \frac{1}{Re} + \frac{1}{Rm} \right), \quad \delta\lambda_{\pm}^H = 0,$$
 (4.2)

where  $h$  is the harmonic mean of the two Reynolds numbers.

### 4.2 Weak ohmic diffusion destabilizes positive energy waves at low $Pm$

In the close vicinity of the critical Rossby number of the Hamilton-Hopf bifurcation  $Ro_c \approx -1.07855$  the real increment  $\delta\lambda^A$  to imaginary eigenvalues  $\lambda_1$  with the negative Krein sign and  $\lambda_2$  with the positive Krein sign are shown in Fig. 3(right) for the fixed  $Rm = 10^3$  and varying  $Pm$  (the fluid Renolds number is calculated as  $Re = Rm/Pm$ ). Remarkably, the eigenvalues with the *positive* Krein sign acquire positive growth rates at  $Pm < 1$  when the electrical resistivity prevails over the kinematic viscosity, whereas the eigenvalues with the *negative* Krein sign become dissipatively-destabilized when  $Pm > 1$ , i.e. when the losses due to viscosity of the fluid exceed the ohmic losses. The interval of negative real increments

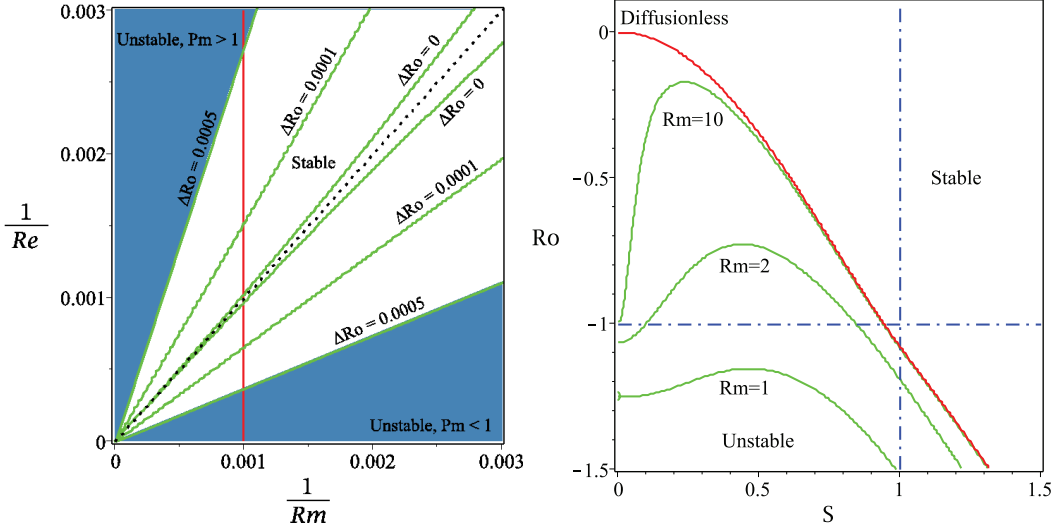


Figure 4: (Left) For  $S = 1$ ,  $Rb = -1$ , and  $n = \sqrt{2}$  the neutral stability curves in the plane  $(Rm^{-1}, Re^{-1})$  of the inverse magnetic and fluid Reynolds numbers corresponding to different values of  $\Delta Ro := Ro - Ro_c$ . Stability domain has a shape of an angle at  $\Delta Ro > 0$  and a cusp at  $\Delta Ro = 0$  with the single tangent line  $Pm = 1$ , cf. Fig 3(right). (Right) The neutral stability curves for  $Rb = -1$ ,  $n = \sqrt{2}$ , and  $Re = Rm$  in the  $(S, Ro)$ -plane at various values of  $Rm$ .

decreases with the decrease in the deviation from the critical value of the Rossby number at the Hamilton-Hopf bifurcation, i.e. as  $\Delta Ro = Ro - Ro_c$  tends to zero. When  $\Delta Ro = 0$ , the stable interval reduces to the single value:  $Pm = 1$ . Hence, weak ohmic diffusion (weak kinematic viscosity) destabilizes positive (negative) energy waves at  $Pm < 1$  ( $Pm > 1$ ), if  $|Ro - Ro_c|$  is sufficiently small.

Note that the destabilizing influence of the kinematic viscosity of the fluid on the negative energy waves is well-known in hydrodynamics [59, 55, 13], which therefore puts the dissipation-induced instability at  $Pm > 1$  and  $|Ro - Ro_c| \ll 1$  into the established context. In contrast, the destabilization of positive energy modes was noticed only in the context of solid mechanics, in particular, in gyroscopic systems with damping and non-conservative positional (or circulatory, or curl [7]) forces in [25, 28, 29]. To the best of our knowledge, the dissipative destabilization of the positive energy modes was never reported in hydrodynamics and MHD.

#### 4.3 Diffusionless and double-diffusive criteria are connected at $Pm = 1$

We complement the sensitivity analysis of eigenvalues of the diffusionless Hamiltonian eigenvalue problem with respect to the double-diffusive perturbation with the direct computation of the stability boundaries based on the algebraic Bilharz stability criterion. The Bilharz criterion [8] guarantees localization of all the roots of a complex polynomial of degree  $n$  to the left of the imaginary axis in the complex plane provided that all principal minors of even order of the  $2n \times 2n$  Bilharz matrix composed of the real and imaginary parts of the coefficients of the polynomial are positive [29].



Applying the Bilharz criterion to the characteristic polynomial of the eigenvalue problem (2.26) we plot the neutral stability curves in the plane of the inverse Reynolds numbers  $\text{Rm}^{-1}$  and  $\text{Re}^{-1}$  at various values of  $\Delta\text{Ro} = \text{Ro} - \text{Ro}_c$ , where  $\text{Ro}_c$  is defined in (3.7), when  $S = 1$ ,  $\text{Rb} = -1$ , and  $n = \sqrt{2}$ , Fig. 4(left). Note that the diagonal ray corresponding to  $\text{Pm} = 1$  stays always in the stability domain when  $\Delta\text{Ro} \geq 0$  and is the only tangent line to the stability boundary at the cuspidal point at the origin when  $\text{Ro} = \text{Ro}_c$ . Moreover, at  $\text{Ro} = \text{Ro}_c$  and  $\text{Re} = \text{Rm}$  the spectrum of the double-diffusive system with  $S = 1$  and  $\text{Rb} = -1$  contains the double complex eigenvalues (exceptional points [29])

$$\lambda_d = \lambda_c(n) - \frac{1}{\text{Rm}}. \quad (4.3)$$

The imaginary eigenvalue  $\lambda_c(n)$  is defined in (3.9) for the particular case of  $n = \sqrt{2}$ .

Approaching the origin along the ray  $\text{Pm} = 1$  means letting the Reynolds numbers tend to infinity with their ratio being kept equal to unity. Fig. 4(right) demonstrates that in the limit  $\text{Re} = \text{Rm} \rightarrow \infty$  the neutral stability curve of the double-diffusive system approaches the threshold of instability of the diffusionless system from below. The instability domain of the double-diffusive system always remains smaller than in the diffusionless case. As a consequence, the Chandrasekhar equipartition solution ( $\text{Ro} = \text{Rb} = -1, S = 1$ ), being stable in the diffusionless case, remains stable at  $\text{Pm} = 1$  no matter what the value of the Reynolds numbers is, Fig. 4(right).

Indeed, in the case when  $\text{Ro} = \text{Rb}S^2$  and  $\text{Re} = \text{Rm}$ , the roots of the characteristic polynomial of the eigenvalue problem (2.26) can be found explicitly

$$\begin{aligned} \lambda_{1,2} &= -i(n+1) - \frac{1}{\text{Rm}} \pm i\sqrt{1 - S^2[1 - (n+1)^2]}, \\ \lambda_{3,4} &= -i(n-1) - \frac{1}{\text{Rm}} \pm i\sqrt{1 - S^2[1 - (n-1)^2]}. \end{aligned} \quad (4.4)$$

The eigenvalues (4.4) are nothing else but the eigenvalues (3.2) that are shifted by dissipation to the left in the complex plane (asymptotic stability). This fact perfectly agrees with the result of Bogoyavlenskij [10] who found at  $\text{Pm} = 1$  exact energy equipartition solutions of the viscous and resistive incompressible MHD equations that relax with the growth rate equal to  $-\frac{1}{\text{Re}} = -\frac{1}{\text{Rm}} < 0$  to the ideal and steady Chandrasekhar equipartition equilibria [14].

## 4.4 Double-diffusive instability at $\text{Pm} \neq 1$ and arbitrary $\text{Re}$ and $\text{Rm}$

### 4.4.1 Unfolding the Hamilton-Hopf bifurcation in the vicinity of $\text{Pm} = 1$

At any  $\text{Re} > 0$ ,  $\text{Rm} > 0$  such that  $\text{Re} = \text{Rm}$  the variation of  $\text{Ro}$  at the given  $\text{Rb} = -1$ ,  $S = 1$ , and  $n$  is accompanied by the bifurcation at  $\text{Ro} = \text{Ro}_c$  of the double complex eigenvalue (4.3) with the negative real part equal to  $-\text{Rm}^{-1}$ , Fig. 5(left). Effectively, at  $\text{Pm} = 1$  dissipation shifts the Hamilton-Hopf bifurcation to the left in the complex plane. By this reason, the oscillatory instability in the double-diffusive system with equal viscosity and resistivity occurs through the Hopf bifurcation at  $\text{Ro}(\text{Rm}) < \text{Ro}_c$  with  $\text{Ro}(\text{Rm})$  tending to  $\text{Ro}_c$  as  $\text{Rm} \rightarrow \infty$ .

In the case when the magnetic Prandtl number slightly deviates from the value  $\text{Pm} = 1$ , the shifted Hamilton-Hopf bifurcation unfolds into a couple of quasi-hyperbolic eigenvalue branches passing close to each other in an avoided crossing centered at an exceptional point

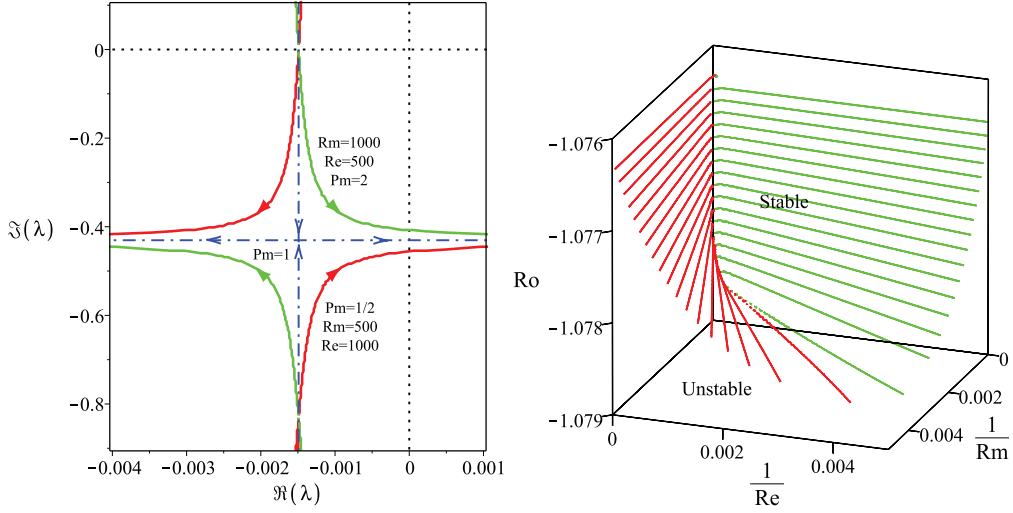


Figure 5: (Left) At  $Rb = -1$ ,  $S = 1$ , and  $n = \sqrt{2}$  the dash-dot lines show interaction of complex eigenvalues with negative real parts in the complex  $\lambda$ -plane with the decrease in  $Ro$  when  $Re = Rm = h = \frac{2}{\frac{1}{500} + \frac{1}{1000}}$ , i.e.  $Pm = 1$ . At  $Ro = Ro_c$  the eigenvalues merge into the double complex eigenvalue (4.3). The quasi-hyperbolic curves demonstrate the imperfect merging of modes (the avoided crossing) such that the mode with the positive Krein (energy) sign becomes unstable at  $Pm < 1$  and the mode with the negative Krein (energy) sign is unstable at  $Pm > 1$ . (Right) The neutral stability surface represented by the contours  $Ro = const.$  in the  $(Re^{-1}, Rm^{-1}, Ro)$ -space has a “Whitney umbrella” singular point at  $(0, 0, Ro_c)$  yielding a cusp in the cross-section  $Ro = Ro_c$  with the single tangent line  $Pm = 1$ .

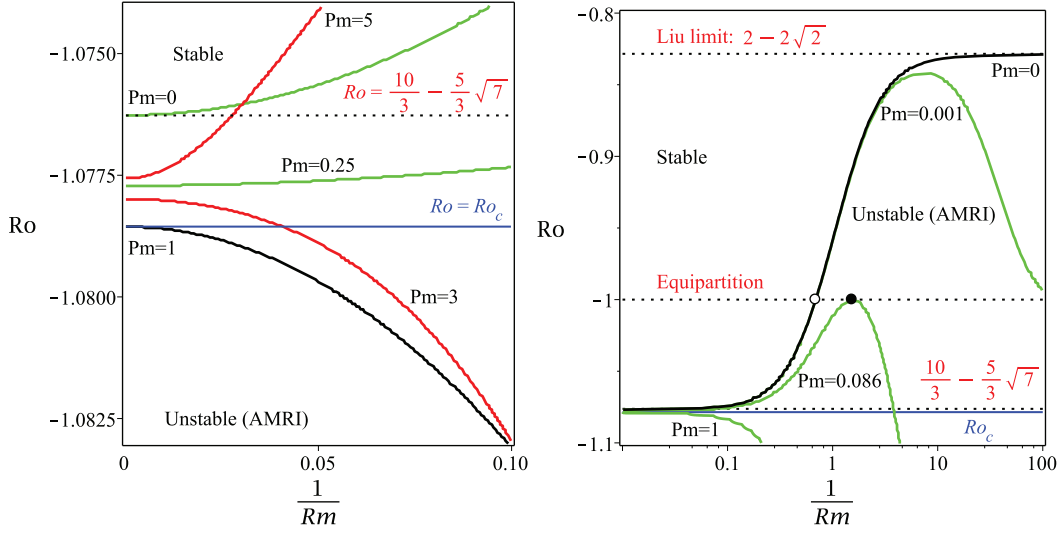


Figure 6: (Left) For  $Rb = -1$ ,  $S = 1$ ,  $n = \sqrt{2}$ , and  $Re = Rm/Pm$  the neutral stability curves in the  $(Rm^{-1}, Ro)$ -plane demonstrating that the limit of the critical value of  $Ro$  as  $Rm \rightarrow \infty$  depends on  $Pm$  and attains its minimum  $Ro_c$  at  $Pm = 1$ . (Right) The neutral stability curves at various  $Pm \in [0, 1]$  demonstrating that the maximal critical values of  $Ro$  do not exceed the Liu limit  $2 - 2\sqrt{2}$  that is attained only at  $Pm = 0$  in the limit of  $Rm \rightarrow 0$ .

$\lambda_d$  of the family (4.3) with the real part equal to  $-h^{-1}$ , where  $h = \frac{2}{\frac{1}{Re} + \frac{1}{Rm}}$  is a harmonic mean of the fluid and magnetic Reynolds numbers,  $Re \neq Rm$ , Fig. 5(left).

The unfolding of the eigenvalue crossing into the avoided crossing can happen in two different ways depending on the sign of  $Pm - 1$ . At  $Pm < 1$  ( $Pm > 1$ ) the complex eigenvalues stemming from the imaginary eigenvalues of the diffusionless system with the positive (negative) Krein sign form a branch that is bending to the right and crossing the imaginary axis at some  $Ro(Re, Rm) \neq Ro_c$ , Fig. 5(left). The critical values  $Ro(Re, Rm)$  of the double-diffusive system live on the surface in the  $(Re^{-1}, Rm^{-1}, Ro)$ -space that has a self-intersection along the  $Ro$ -axis, Fig. 5(right). The angle of the self-intersection tends to zero as  $Ro \rightarrow Ro_c$  and at the point  $(0, 0, Ro_c)$  the surface has a singularity known as the Whitney umbrella [34, 26, 3].

In the vicinity of the  $Ro$ -axis the instability threshold is effectively a ruled surface [11], the slope of a ruler is determined by  $Pm$ . Tending the Reynolds numbers to infinity while keeping the magnetic Prandtl number fixed results in the approaching the  $Ro$ -axis in the  $(Re^{-1}, Rm^{-1}, Ro)$ -space along a ruler corresponding to this value of  $Pm$ . Generically, for all values of  $Pm$  but  $Pm = 1$  a ruler leads to a limiting value of  $Ro$  that exceeds  $Ro_c$  and thus extends the instability interval of the fluid Rossby numbers with respect to that of the diffusionless system, as is visible in Fig. 5(right) and Fig. 6(left). The plane  $Pm = 1$  divides the neutral stability surface in the vicinity of  $Ro = Ro_c$  into two parts corresponding to positive energy modes destabilized by the dominating ohmic diffusion at  $Pm < 1$  and to negative energy modes destabilized by the dominating fluid viscosity at  $Pm > 1$ , Fig. 5(right). The ray determined by the conditions  $Re = Rm > 0$ ,  $Ro = Ro_c$  belongs to the stability domain of the double-diffusive system and contains exceptional

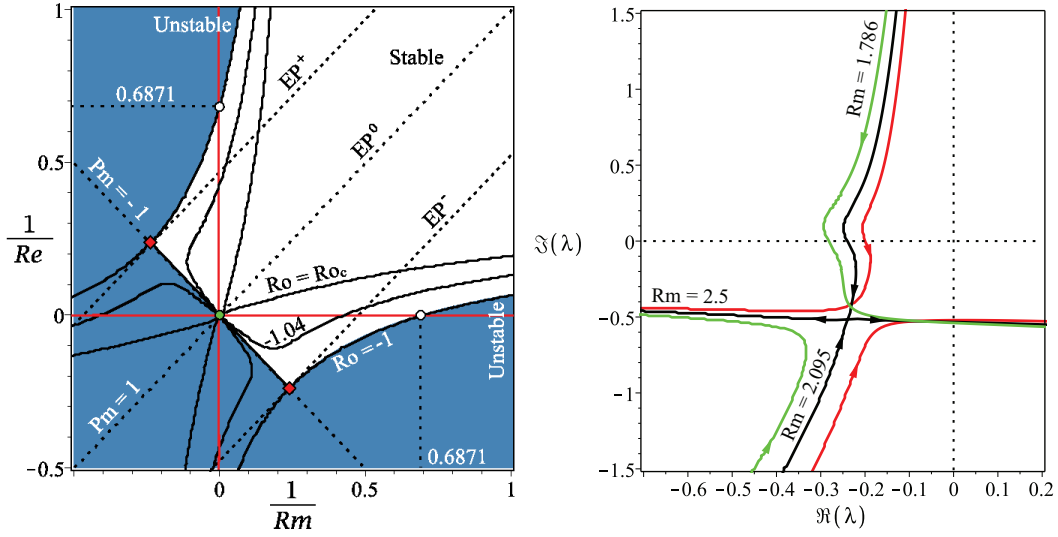


Figure 7: (Left) Contour plots of the neutral stability surface in the plane of inverse Reynolds numbers at (cuspidal curve)  $Ro = Ro_c \approx -1.07855$ , (filled area)  $Ro = -1$ , and (intermediate curve)  $Ro = -1.04$ . Two singular Whitney umbrella points (filled diamonds) exist at the intersection of the line  $Pm = -1$  and the neutral stability curve at  $Ro = -1$  and another one exists at the origin when  $Ro = Ro_c$ . From these singularities the lines  $EP^\pm, EP^0$  of exceptional points are stemming that govern the transfer of modes shown in the right panel. (Right) For  $Rb = -1$ ,  $S = 1$ ,  $n = \sqrt{2}$ , and  $Re = 1000$  the movement of eigenvalues with the decrease in  $Ro$  at various  $Rm$  chosen such that  $Pm < 1$ . At  $Rm < 1000$  and up to  $Rm = Rm_{EP-} \approx 2.095$  it is the branch corresponding to perturbed imaginary eigenvalues with the positive Krein sign that causes instability. When  $Rm = Rm_{EP-}$  two simple eigenvalues approach each other to merge exactly at  $Ro = -1$  into a double eigenvalue with the Jordan block,  $\lambda_{EP-} \approx -i0.5086 - 0.2391$ . At  $Rm < Rm_{EP-}$  the instability transfers to the branch corresponding to perturbed imaginary eigenvalues with the negative Krein sign.

points (4.3) that determine<sup>4</sup> behaviour of eigenvalues shown in Fig. 5(left).

Fig. 6(left) shows that at a fixed  $Pm \neq 1$  the critical value of  $Ro$  at the onset of the double-diffusive AMRI is displaced by an order one distance along the  $Ro$ -axis with respect to the critical value  $Ro_c$  of the diffusionless case, when both viscous and ohmic diffusion tend to zero. Nevertheless, this displacement is rather small if  $Pm \in [0, 1]$  with the maximum attained at  $Pm = 0$  where the diffusionless limit of the critical Rossby number is equal to  $\frac{5}{3}(2 - \sqrt{7}) \approx -1.07625 < -1$ , i.e. weak dissipation with dominating ohmic losses is not capable to destabilize even the Chandrasekhar equipartition solution at  $Ro = -1$ . Does the increase in viscosity and resistivity change this tendency?

<sup>4</sup>Quite in accordance with anticipations of Jones [24]: "It is quite common for an eigenvalue which is moving steadily towards a positive growth rate to suffer a sudden change of direction and subsequently fail to become unstable; similarly, it happens that modes which initially become more stable as [the Reynolds number] increases change direction and subsequently achieve instability. It is believed that these changes of direction are due to the nearby presence of multiple-eigenvalue points."

#### 4.4.2 AMRI of the Rayleigh-stable flows at low and high Pm when dissipation is finite

Indeed, it does. Fig. 6(right) demonstrates the evolution of the critical Rossby number as a function of  $Rm^{-1} \in [0, 100]$  under the constraint  $Rm - RePm = 0$  at various  $Pm \in [0, 1]$  in the assumption that  $Rb = -1$ ,  $S = 1$ , and  $n = \sqrt{2}$ . Despite the critical Rossby number does not exceed the value  $Ro = -1$  of the equipartition solution for all  $Pm \in [0, 1]$  when  $Rm^{-1} < 0.1$ , it can grow considerably and attain a maximum when  $Rm^{-1} > 0.1$ . For instance, if  $Pm = Pm_l \approx 0.0856058$  the maximal critical value is  $Ro = -1$ , which is attained at  $Rm = Rm_l \approx 0.6552421$  (or  $Rm_l^{-1} \approx 1.5261535$ ), see Fig. 6(right) where this maximum is marked by the filled circle. For  $0 < Pm < Pm_l$  the maximal critical Rossby number exceeds the value of  $Ro = -1$ .

In the inductionless limit ( $Pm = 0$ ) the azimuthal magnetorotational instability (AMRI) occurs at  $Ro \geq -1$  if  $Rm \leq Rm_*$ , where  $Rm_* = \frac{1}{2}\sqrt{4 + 2\sqrt{5}}$  ( $Rm_*^{-1} \approx 0.6871$ , open circle in Fig. 6(right)). The critical value of the fluid Rossby number monotonously grows with the decrease in  $Rm$  attaining its maximal value<sup>5</sup>  $Ro^- = 2 - 2\sqrt{2} \approx -0.8284$  at  $Rm = 0$ .

If  $Ro = Rb$ ,  $S = 1$ , then at  $Pm = 0$  we have

$$Rm_*^2 = \frac{n^2(n^4 - 12Rb^2 + 16Rb) - 16(Rb + 2)(Rb^2 - n^2) - n((n^2 - 2Rb)^2 + 8(Rb^2 - n^2))\sqrt{n^2 + 8Rb + 16}}{32(Rb^2 - n^2)(n^2 - Rb - 2)^2}, \quad (4.5)$$

in agreement with the results of [30]. At  $Rb = -1$  and  $n = \sqrt{2}$  Eq. (4.5) yields  $Rm_* = \frac{1}{2}\sqrt{4 + 2\sqrt{5}}$ .

On the other hand, the lower Liu limit as a function of  $n$  and  $Rb$  is [30]:

$$Ro^-(n, Rb) = -2 + (n^2 - 2Rb) \frac{n^2 - 2Rb - \sqrt{(n^2 - 2Rb)^2 - 4n^2}}{2n^2}. \quad (4.6)$$

Note that  $Ro^-(n, Rb)$  attains its maximum  $2 - 2\sqrt{2}$  at  $n = \sqrt{-2Rb}$ , which explains our choice of  $n = \sqrt{2}$  for the case when  $Rb = -1$ , cf. also Fig. 1(right). Moreover, at  $n = \sqrt{-2Rb}$  the instability condition  $Ro < Ro^-$  reduces to (1.11) after some algebra.

We see that there exists a critical value of the magnetic Prandtl number  $Pm_l < 1$  such that at  $Pm \in [0, Pm_l]$  the Chandrasekhar equipartition solution with  $Rb = Ro = -1$ , and  $S = 1$  is destabilized by dissipation when viscosity is sufficiently small and ohmic diffusion is sufficiently large. In contrast, at  $Ro - Ro_c \ll 1$  the marginally stable diffusionless system can be destabilized at  $Pm < 1$  when both viscosity and resistivity is infinitesimally small, Fig. 4(left).

In order to understand how these instabilities are related to each other, we plot the neutral stability curves in the plane of inverse Reynolds numbers  $Re^{-1}, Rm^{-1} \in [-0.5, 1]$  for  $Ro \in [Ro_c, -1]$ , Fig. 7(left). Although the negative Reynolds numbers have no physical meaning, it is instructive to extend the neutral stability curves to the corresponding region of the parameter plane. At  $Ro = Ro_c$  the stability domain is inside the area bounded by a curve having a cuspidal singularity at the origin with the tangent line at the cuspidal point specified by the condition  $Pm = 1$ ; this geometry yields destabilization by infinitesimally small dissipation at all  $Pm \neq 1$ .

As soon as  $Ro$  departs from  $Ro_c$ , the cusp at the origin transforms into a self-intersection, the angle of which increases with the increase in  $Ro$  and becomes equal to  $\pi$  at  $Ro = -1$ . By

---

<sup>5</sup>known as the lower Liu limit [37, 30, 17]

this reason, at  $Ro$  close to  $-1$  the neutral stability curve partially belongs to the region of negative Reynolds numbers which makes destabilization by infinitesimally small dissipation impossible for all  $Pm > 0$ . In particular, at  $S = 1$  and vanishing viscosity the ohmic diffusion is stabilizing in the interval  $0 < Rm^{-1} < Rm_*^{-1}$  when

$$Ro > Ro_{Rm} := \frac{6Rb^2 - Rbn^2 + 6n^2 - 2(n^2 - 3Rb)\sqrt{Rb^2 + 3n^2}}{3n^2}. \quad (4.7)$$

At  $Rb = -1$  and  $n = \sqrt{2}$  we have  $Ro_{Rm} = \frac{5}{3}(2 - \sqrt{7}) \approx -1.07625 > Ro_c \approx -1.07855$ . At  $S = 1$  and  $Ro = Rb$  the critical magnetic Reynolds number  $Rm_*$  is defined by Eq. (4.5).

A similar instability domain exists also in the case of  $Pm > 1$ , Fig. 7(left). At  $Ro = -1$  the ray from the origin with the slope  $Pm = Pm_u \approx 11.681451$  is tangent to the boundary of the domain at  $Re = Re_u \approx 0.6552421$  ( $Re_u^{-1} \approx 1.5261535$ ). In particular, in the case of vanishing ohmic dissipation the instability occurs at  $Re < Re_*$  when  $Ro > Ro_{Re}$ , where  $Re_*$  is given by

$$Re_*^2 = \frac{n^6 - 4(Rb+1)n^4 - 4Rb^2(3n^2 + 4Rb + 8) + n(4(Rb+2)^2 - (n^2 - 2)^2 - 12)\sqrt{n^2 - 8Rb}}{32((Rb+2)^2 - n^2)(n^2 + Rb)^2}. \quad (4.8)$$

At  $Rb = -1$  and  $n = \sqrt{2}$  we have  $Ro_{Re} \approx -1.07639$  and  $Re_* = \frac{1}{2}\sqrt{4 + 2\sqrt{5}} = Rm_*$ .

Hence, the Chandrasekhar equipartition solution ( $Ro = Rb = -1, S = 1$ ) can be destabilized by dissipation either when  $0 \leq Pm < Pm_l$  and  $0 < Rm < Rm_*$  or when  $Pm_u < Pm < \infty$  and  $0 < Re < Re_*$ , see Fig. 7(left) where open circles mark the values of  $Re_*$  and  $Rm_*$ . At  $n = \sqrt{2}$  stability of the Chandrasekhar solution is not affected by the double diffusion if  $Pm \in [0.0856058, 11.681451]$ .

#### 4.4.3 Transfer of instability between modes when $Pm$ significantly deviates from 1

Fig. 7(left) shows that the neutral stability curves at  $Ro = -1$  orthogonally intersect the anti-diagonal line with the slope  $Pm = -1$  at the two exceptional points (marked by the filled diamonds) with the coordinates  $(Rm_\diamond^{-1}, -Re_\diamond^{-1})$  and  $(-Rm_\diamond^{-1}, Re_\diamond^{-1})$ , where

$$Rm_\diamond^{-1} = Re_\diamond^{-1} = \frac{\sqrt{2}}{4n} \sqrt{8n^4 + 20n^2 - 1 - (8n^2 + 1)^{3/2}}. \quad (4.9)$$

At the both exceptional points there exists a pair of simple imaginary eigenvalues and a double imaginary eigenvalue  $\lambda_\diamond$  with the Jordan block:

$$\lambda_\diamond = -i \frac{4n^2 - 1 - \sqrt{1 + 8n^2}}{4n}. \quad (4.10)$$

At  $n = \sqrt{2}$  Eqs. (4.9) and (4.10) yield

$$Rm_\diamond^{-1} = Re_\diamond^{-1} = \frac{1}{4} \sqrt{71 - 17\sqrt{17}} \approx 0.23811, \quad \lambda_\diamond = -i \frac{7 - \sqrt{17}}{4\sqrt{2}} \approx -i0.50857. \quad (4.11)$$

A segment of the anti-diagonal between the exceptional points is a part of the stability boundary at  $Ro = -1$  and all the eigenvalues at the points of this segment are imaginary.

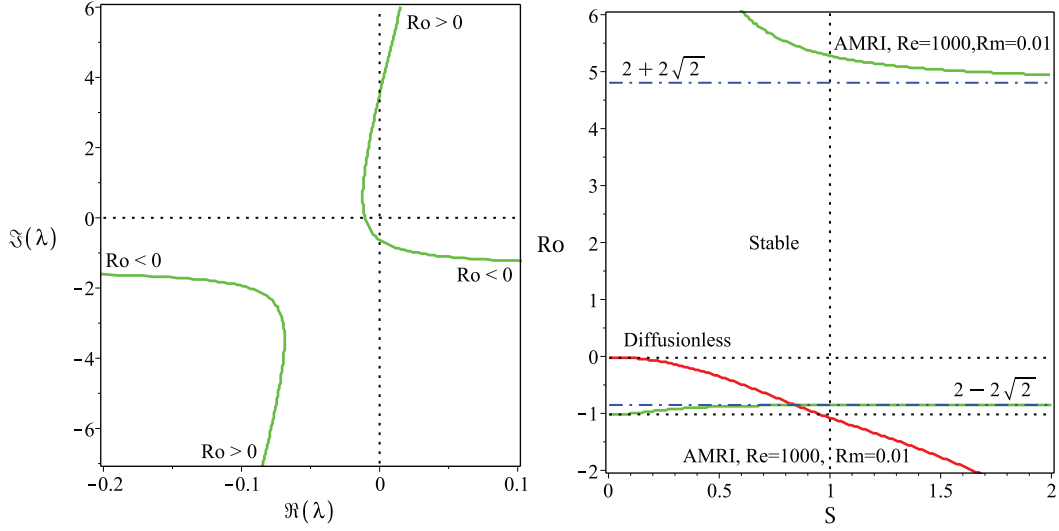


Figure 8: (Left) For  $Rb = -1$ ,  $S = 1$ , and  $n = \sqrt{2}$  and fixed  $Re = 1000$  and  $Rm = 0.01$  the movement of eigenvalues in the complex plane with the variation in  $Ro$  demonstrating that at  $Pm = 10^{-5}$  one and the same eigenvalue branch is responsible for instability both at  $Ro < 0$  and  $Ro > 0$ . (Right) The corresponding neutral stability curves in the  $(S, Ro)$ -plane exist below the lower Liu limit of  $Ro = 2 - 2\sqrt{2}$  (destabilizing the Chandrasekhar equipartition solution) and above the upper Liu limit of  $Ro = 2 + 2\sqrt{2}$  that are attainable only at  $Re \rightarrow \infty$  and  $Rm \rightarrow 0$ . In contrast, the diffusionless AMRI exists above the lower Liu limit at small  $S$  but does not affect the Chandrasekhar equipartition solution at  $S = 1$ .



We see that the domain of asymptotic stability at  $Ro = -1$  extends to the region of negative Reynolds numbers and that at the constraint  $Rm = -Re$  the double-diffusive system has imaginary spectrum on the interval between the two exceptional points. If we interpret the negative dissipation as an energy gain, then, formally, we could say that at  $Rm = -Re$  the energy gain is compensated by the energy loss. Non-Hermitian systems with the balanced gain and loss are known as the parity-time (PT) symmetric systems [28, 51]. The interval of marginal stability of the PT-symmetric system forms a self-intersection singularity on the stability boundary of a general dissipative system with the Whitney umbrella singularities at the exceptional points corresponding to double imaginary eigenvalues [28, 29]. Therefore, the neutral stability surface of our double-diffusive system contains the interval of self-intersection on the  $Ro$ -axis ( $Ro > Ro_c$ ) that is orthogonal at  $Ro = -1$  to the interval of the anti-diagonal with the slope  $Pm = -1$  confined between the two exceptional points. At the exceptional points of this interval and at the exceptional point on the  $Ro$ -axis at  $Ro = Ro_c$  the neutral stability surface in the  $(Rm^{-1}, Re^{-1}, Ro)$ -space has three Whitney umbrella singularities. The singularities ‘hidden’ in the region of negative Reynolds numbers are responsible for the separation of domains of AMRI due to weak or strong dissipation.

It turns out, that this separation is not only quantitative but also qualitative, as comparison of the movement of eigenvalues demonstrates at the fixed  $Re = 1000$  and  $Rm = 500$  in Fig. 5(left) and at  $Re = 1000$  and  $Rm \approx 1.789$  in Fig. 7(right). In both cases  $Pm < 1$ . However, in the case of  $Pm = 0.5$  it is the branch with the lower negative frequencies corresponding to the perturbed imaginary eigenvalues with the positive Krein sign of the diffusionless Hamiltonian system that becomes unstable due to prevailing ohmic diffusion. In contrast, at much smaller  $Pm \approx 0.001789$  the instability transfers to a branch with the higher negative frequencies that can be seen as stemming from the imaginary eigenvalues with the negative Krein sign of the diffusionless Hamiltonian system. Keeping  $Re = 1000$  and slightly increasing the magnetic Reynolds number to  $Rm \approx 2.095$  we see at  $Ro = -1$  the crossing of the eigenvalue branches at the double eigenvalue  $\lambda_{EP-} \approx -i0.5086 - 0.2391$ . The crossing transforms into another avoided crossing when  $Rm = 2.5$ . At  $Rm = 2.5$ , again, it is the branch corresponding to higher negative frequencies (positive Krein sign) that is destabilized by dissipation, Fig. 7(right).

In fact, when  $Re = 1000$  is given, the branch corresponding to the unperturbed imaginary eigenvalues with the positive Krein sign is destabilized by dissipation when the magnetic Reynolds number decreases from  $Rm = 1000$  ( $Pm = 1$ ) to  $Rm \approx 2.095$  ( $Pm \approx 0.002095$ ). As soon as  $Rm < 2.095$  ( $Pm < 0.002095$ ) the instability transfers to a branch corresponding to the unperturbed imaginary eigenvalues with the negative Krein sign. The reason is the existence of a set in the stability domain corresponding to double complex eigenvalues. This set exists at  $Ro = -1$  and consists of the two straight lines

$$\frac{1}{Re} = \pm \frac{2}{Re_\diamond} + \frac{1}{Rm} \quad (4.12)$$

that are tangent to the neutral stability curves at the exceptional points with the coordinates  $(Rm_\diamond^{-1}, -Re_\diamond^{-1})$  and  $(-Rm_\diamond^{-1}, Re_\diamond^{-1})$ , where  $Rm_\diamond$  and  $Re_\diamond$  are defined by Eq. (4.9).

In Fig. 7(left) the lines corresponding to different sign in Eq. (4.12) are marked as  $EP^+$  (the upper dot line) and  $EP^-$  (the lower dot line). At the points of the EP-lines (4.12)

there exist double complex eigenvalues (exceptional points)  $\lambda_{\text{EP}\pm}$  given by the expression

$$\lambda_{\text{EP}\pm} = \lambda_{\diamond} - \left( \frac{1}{\text{Rm}} \pm \frac{1}{\text{Rm}_{\diamond}} \right). \quad (4.13)$$

At  $n = \sqrt{2}$  and  $\text{Re}_{\text{EP}^-} = 10^3$ , we find that  $\frac{1}{\text{Rm}_{\text{EP}^-}} = \frac{2}{\text{Re}_{\diamond}} + \frac{1}{\text{Re}_{\text{EP}^-}} \approx 0.477$  ( $\text{Rm}_{\text{EP}^-} \approx 2.095$ ) and

$$\lambda_{\text{EP}^-} = i \frac{\sqrt{17} - 7}{4\sqrt{2}} - \frac{1}{4} \sqrt{71 - 17\sqrt{17}} - \frac{1}{\text{Re}_{\text{EP}^-}} \approx -0.2391 - i0.5086. \quad (4.14)$$

We see that the three Whitney umbrella points and related to them three lines of double complex eigenvalues (marked in Fig. 7(left) as  $\text{EP}^{\pm}$  and  $\text{EP}^0$ ) actually control the dissipation-induced destabilization acting as switches of unstable modes. The singular geometry of the neutral stability surface guides the limiting scenarios and connection of the double-diffusive system to a Hamiltonian or to a PT-symmetric one.

#### 4.4.4 Connection between the lower and upper Liu limits at $\text{Pm} \ll 1$

Let us keep  $\text{Re} = 1000$  and allow the magnetic Reynolds number to decrease beyond the critical value  $\text{Rm}_{\text{EP}^-} \approx 2.095$ . During this process the pattern of interacting eigenvalues remains qualitatively the same, cf. Fig. 7(right) and Fig. 8(left). However, a new important feature appears as the magnetic Prandtl number approaches the inductionless limit  $\text{Pm} = 0$ . Indeed, at  $\text{Re} = 1000$  and  $\text{Rm} = 0.01$  corresponding to  $\text{Pm} = 10^{-5}$  one and the same eigenvalue branch has unstable parts both at  $\text{Ro} < 0$  and at  $\text{Ro} > 0$ , see Fig. 8(left). This is in striking contrast to the case of moderately small magnetic Prandtl numbers shown in Fig. 7(right) or to the diffusionless case when the instability occurs only at  $\text{Ro} < 0$ .

The Bilharz criterion reveals two regions of instability in the  $(S, \text{Ro})$ -plane for  $\text{Rb} = -1$ ,  $n = \sqrt{2}$  and  $\text{Re} = 1000$  and  $\text{Rm} = 0.01$ , Fig. 8(right). The first one exists at  $\text{Ro} < 2 - 2\sqrt{2} < 0$  and the second one at  $\text{Ro} > 2 + 2\sqrt{2} > 0$ . In the gap between the lower Liu limit ( $2 - 2\sqrt{2}$ ) and the upper Liu limit ( $2 + 2\sqrt{2}$ ) the system is stable [30, 37]. The both Liu limits are attained when  $\text{Re} \rightarrow \infty$  and  $\text{Rm} \rightarrow 0$ . If the double-diffusive instability domain at  $\text{Ro} < 0$  can be considered as a deformation of the instability domain of the diffusionless system, the instability of the magnetized circular Couette flow in super rotation [52] at  $\text{Ro} > 0$  turns out to be an effect existing only in the presence of dissipation. Remarkably, the two seemingly different instabilities are caused by the eigenvalues living on one and the same eigenvalue branch in the complex plane, Fig. 8(left).

The oscillatory instability at  $\text{Pm} \ll 1$  of a circular Couette flow in an azimuthal magnetic field with  $\text{Rb} = -1$  and  $\text{Ro} < 2 - 2\sqrt{2}$ , i.e. the azimuthal magnetorotational instability (AMRI), has already been observed in recent experiments with liquid metals [49]. We therefore identify the observed *inductionless AMRI at  $\text{Pm} \ll 1$  as nothing else but the manifestation of a dissipation-induced instability of the waves of negative energy of the diffusionless system caused by the prevailing ohmic diffusion*. In particular, at  $\text{Ro} = \text{Rb} = -1$  and  $S = 1$  the inductionless AMRI is the dissipation-induced instability of the Chandrasekhar equipartition solution.

## 5 Conclusion

We have studied azimuthal magnetorotational instability (AMRI) of a circular Couette flow of an incompressible electrically conducting Newtonian fluid in the presence of the azimuthal magnetic field of arbitrary radial dependence. With the use of the geometrical optics asymptotic solutions we have reduced the problem to the analysis of the dispersion relation of the transport equation for the amplitude of the localized perturbation. We have represented the corresponding matrix eigenvalue problem in the form of a Hamiltonian diffusionless system perturbed by the ohmic diffusion and fluid viscosity. We have established that the diffusionless AMRI corresponds to the Krein collision of simple imaginary eigenvalues with the opposite Krein (or energy) sign and derived an analytical expression for the instability threshold of the diffusionless system with the use of the discriminant of the complex polynomial dispersion relation. We have demonstrated that the threshold of the double-diffusive AMRI with equal contribution of viscosity and electrical resistivity ( $Pm = 1$ ) smoothly converges to the threshold of the diffusionless AMRI in the limit of the infinitesimally small dissipation.

Contrary to the case when the coefficients of viscosity and resistivity are equal, the prevalence of resistivity over viscosity or vice-versa causes the azimuthal magnetorotational instability in the parameter regions where the diffusionless AMRI is prohibited, for instance, in the case of super-rotating flows. In particular, non-equal viscosity and resistivity destabilize the celebrated Chandrasekhar energy equipartition solution. Analyzing the neutral stability surface of the double-diffusive system we have found that:

- marginally stable Hamiltonian equilibria of the diffusionless system form an edge on the neutral stability surface of the double-diffusive system that ends up with the Whitney umbrella singular point at the onset of the Hamilton-Hopf bifurcation;
- another edge with the two Whitney umbrella singular points at its ends corresponds to marginally stable double-diffusive systems with the balanced energy gain and loss (PT-symmetric systems);
- three codimension-2 sets corresponding to complex double-degenerate eigenvalues with the Jordan block (exceptional points) are stemming from each of the Whitney umbrella singularities and live in the stability domain of the double-diffusive system;
- the sets of exceptional points control transfer of instability between modes of positive and negative energy whereas the Whitney umbrellas govern the limiting scenarios for the instability thresholds including the case of vanishing dissipation;
- AMRI is the dissipation-induced instability of the Chandrasekhar equipartition solution when either  $Pm \in [0, 1)$  is sufficiently small or  $Pm \in (1, \infty)$  is sufficiently large.
- inductionless AMRI occurring both at  $Ro < 0$  and  $Ro > 0$  when  $Pm \ll 1$  is caused by the eigenvalues of the one and the same branch stemming from the negative energy modes of the diffusionless system, i.e. it is a classical dissipation-induced instability.

The author is thankful for partial support through the EU FP7 ERC grant ERC-2013-ADG-340561-INSTABILITIES.

## References

- [1] Acheson DJ. 1978. On the instability of toroidal magnetic fields and differential rotation in stars. *Phil. Trans. R. Soc. London. Ser. A, Math. Phys. Sci.* **289**(1363), 459–500.
- [2] Allilueva AI, Shafarevich AI. 2015. Asymptotic solutions of linearized Navier-Stokes equations localized in small neighborhoods of curves and surfaces. *Russian J. Math. Phys.* **22**(4), 421–436.
- [3] Arnold VI. 1971. On matrices depending on parameters. *Russ. Math. Surv.* **26**, 29–43.
- [4] Balbus SA, Hawley JF. 1992. A powerful local shear instability in weakly magnetized disks 4. Nonaxisymmetric perturbations. *Astrophys. J.* **400**, 610–621.
- [5] Balbus SA, Henri P. 2008. On the magnetic Prandtl number behavior of accretion disks. *Astrophys. J.* **674**, 408–414.
- [6] Balbus SA, Potter WJ. 2016 Surprises in astrophysical gasdynamics. *Rep. Prog. Phys.* **79**(6), 066901.
- [7] Berry MV, Shukla P. 2015 Hamiltonian curl forces. *Proc. R. Soc. A* **471** 20150002.
- [8] Bilharz H. 1944. Bemerkung zu einem Satze von Hurwitz. *Z. Angew. Math. Mech.* **24**, 77–82.
- [9] Bloch AM, Krishnaprasad PS, Marsden JE, Ratiu TS. 1994. Dissipation-induced instabilities. *Annales de L’Institut Henri Poincaré - Analyse Non-Lineaire.* **11**, 37–90.
- [10] Bogoyavlenskij OI. 2004. Unsteady equipartition MHD solutions. *J. Math. Phys.* **45**, 381–390.
- [11] Bottema O. 1956. The Routh-Hurwitz condition for the biquadratic equation. *Indag. Math.* **59**, 403–406.
- [12] Brandenburg A. 2011. Dissipation in dynamos at low and high magnetic Prandtl numbers. *Astron. Nachr.* **332**(1), 51–56.
- [13] Bridges TJ, Dias F. 2007. Enhancement of the Benjamin-Feir instability with dissipation. *Physics of Fluids* **19**, 104104.
- [14] Chandrasekhar S. 1956. On the stability of the simplest solution of the equations of hydromagnetics. *Proc. Natl. Acad. Sci. U.S.A.* **42**, 273–276.
- [15] Chandrasekhar S. 2010. *A scientific autobiography: S. Chandrasekhar, K. C. Wali, ed.* Singapore: World Scientific.
- [16] Chefranov SG. 2016. Cyclone–anticyclone vortex asymmetry mechanism and linear Ekman friction. *J. Exp. Theor. Phys - JETP* **122**(4), 759–768.
- [17] Child A, Kersalé E, Hollerbach R. 2015. Nonaxisymmetric linear instability of cylindrical magnetohydrodynamic Taylor-Couette flow. *Phys. Rev. E* **92**, 033011.

- [18] Eckhardt B, Yao D. 1995. Local stability analysis along Lagrangian paths. *Chaos, Solitons and Fractals* **5**(11), 2073–2088.
- [19] Eckhoff KS. 1987. Linear waves and stability in ideal magnetohydrodynamics. *Phys. Fluids*, **30**, 3673–3685.
- [20] Friedlander S, Vishik MM. 1995. On stability and instability criteria for magnetohydrodynamics. *Chaos* **5**, 416–423.
- [21] Golovin SV, Krutikov MK. 2012. Complete classification of stationary flows with constant total pressure of ideal incompressible infinitely conducting fluid. *J. Phys. A: Math. Theor.* **45**, 235501.
- [22] Holopäinen EO. 1961. On the effect of friction in baroclinic waves. *Tellus* **13**, 363–367.
- [23] Ji H, Balbus S. 2013. Angular momentum transport in astrophysics and in the lab. *Physics Today, August 2013*, 27–33.
- [24] Jones JA. 1988. Multiple eigenvalues and mode classification in plane Poiseuille flow. *Quart. J. Mech. Appl. Math.*, **41**, 363–382.
- [25] Kirillov ON. 2009. Campbell diagrams of weakly anisotropic flexible rotors. *Proc. R. Soc. A*, **465**, 2703–2723.
- [26] Kirillov ON, Verhulst F. 2010. Paradoxes of dissipation-induced destabilization or who opened Whitney’s umbrella? *Z. Angew. Math. Mech.* **90**(6), 462–488.
- [27] Kirillov ON, Stefani F. 2013. Extending the range of the inductionless magnetorotational instability. *Phys. Rev. Lett.* **111**, 061103.
- [28] Kirillov ON. 2013. Stabilizing and destabilizing perturbations of PT-symmetric indefinitely damped systems. *Phil. Trans. R. Soc. A* **371**, 20120051.
- [29] Kirillov ON. 2013. *Nonconservative stability problems of modern physics*, De Gruyter Studies in Mathematical Physics 14. Berlin, Boston: De Gruyter.
- [30] Kirillov ON, Stefani F, Fukumoto Y. 2014. Local instabilities in magnetized rotational flows: A short-wavelength approach. *J. Fluid Mech.* **760**, 591–633.
- [31] Krechetnikov R, Marsden JE. 2007. Dissipation-induced instabilities in finite dimensions. *Rev. Mod. Phys.* **79**, 519–553.
- [32] Kucherenko VV, Kryvko A. 2013. Interaction of Alfvén waves in the linearized system of magnetohydrodynamics for an incompressible ideal fluid. *Russ. J. Math. Phys.* **20**(1), 56–67.
- [33] Lamb H. 1908. On kinetic stability. *Proc. R. Soc. London A* **80**(537), 168–177.
- [34] Langford WF. 2003. *Hopf meets Hamilton under Whitney’s umbrella*, in: S. N. Namachchivaya, (ed.), IUTAM Symposium on Nonlinear Stochastic Dynamics. Proceedings of the IUTAM Symposium, Monticello, IL, USA, Augsut 26-30, 2002, Solid Mech. Appl. 110, pp. 157–165, Dordrecht: Kluwer.

- [35] Lifschitz A. 1991. Short wavelength instabilities of incompressible three-dimensional flows and generation of vorticity. *Phys. Lett. A* **157**, 481–487.
- [36] Lifschitz A, Suters WH, Beale JT. 1996. The onset of instability in exact vortex rings with swirl. *J. Comp. Phys.* **129**, 8–29.
- [37] Liu W, Goodman J, Herron I, Ji H. 2006. Helical magnetorotational instability in magnetized Taylor-Couette flow. *Phys. Rev. E* **74**(5), 056302.
- [38] MacKay RS. 1991. Movement of eigenvalues of Hamiltonian equilibria under non-Hamiltonian perturbation. *Phys. Lett. A* **155**, 266–268.
- [39] Maddocks JH, Overton ML. 1995. Stability theory for dissipatively perturbed Hamiltonian-systems. *Comm. Pure Appl. Math.* **48**, 583–610.
- [40] Maeder A, Meynet G, Lagarde N, Charbonnel C. 2013. The thermohaline, Richardson, Rayleigh-Taylor, Solberg-Hoiland, and GSF criteria in rotating stars. *Astronomy & Astrophysics* **553** A1-A7.
- [41] Maréchal L, Perez J. 2010. Radial orbit instability as a dissipation-induced phenomenon. *Mon. Not. R. Astron. Soc.* **405**, 2785–2790.
- [42] Michael DH. 1954. The stability of an incompressible electrically conducting fluid rotating about an axis when current flows parallel to the axis. *Mathematika* **1**, 45–50.
- [43] Ilgisonis VI, Khalzov IV, Smolyakov AI. 2008. Negative energy waves and MHD stability of rotating plasmas. *Nucl. Fusion* **49**, 035008.
- [44] Montgomery M. 1993. Hartmann, Lundquist, and Reynolds: The role of dimensionless numbers in nonlinear magnetofluid behavior. *Plasma Phys. Control. Fusion* **35**, B105–B113.
- [45] Morrison PJ, Greene JM. 1980. Noncanonical Hamiltonian density formulation of hydrodynamics and ideal magnetohydrodynamics. *Phys. Rev. Lett.* **45**, 790–794.
- [46] Ogilvie GI, Pringle JE. 1996. The non-axisymmetric instability of a cylindrical shear flow containing an azimuthal magnetic field. *Mon. Not. R. Astron. Soc.* **279**, 152–164.
- [47] Rayleigh JWS. 1917. On the dynamics of revolving fluids. *Proc. R. Soc. Lond. A* **93** 148–154.
- [48] Rüdiger G, Schultz M., Stefani F., Mond M. 2015. Diffusive magnetohydrodynamic instabilities beyond the Chandrasekhar theorem. *Astrophys. J.* **811**(2), 84.
- [49] Seilmayer M, Galindo V, Gerbeth G, Gundrum T, Stefani F, Gellert M, Rüdiger G, Schultz M, Hollerbach R. 2014. Experimental evidence for non-axisymmetric magnetorotational instability in an azimuthal magnetic field. *Phys. Rev. Lett.* **113**, 024505.
- [50] Smith DM. 1933. The motion of a rotor carried by a flexible shaft in flexible bearings. *Proc. R. Soc. Lond. A* **142**, 92–118.

- [51] Schindler J, Li A, Zheng MC, Ellis FM, Kottos T. 2011 Experimental study of active LRC circuits with PT symmetries. *Phys. Rev. A* **84**, 040101(R).
- [52] Stefani F, Kirillov ON. 2015. Destabilization of rotating flows with positive shear by azimuthal magnetic fields. *Physical Review E* **92**, 051001(R).
- [53] Squire J, Bhattacharjee A. 2014. Nonmodal growth of the magnetorotational instability. *Phys. Rev. Lett.* **113**, 025006.
- [54] Swaters GE. 2010. Modal interpretation for the Ekman destabilization of inviscidly stable baroclinic flow in the Phillips model. *J. Phys. Oceanogr.* **40**, 830–839.
- [55] Thorpe SA, Smyth WD, Li L. 2013. The effect of small viscosity and diffusivity on the marginal stability of stably stratified shear flows. *J. Fluid Mech.* **731**, 461–476.
- [56] Turner JS. 1974. Double-diffusive phenomena. *Annu. Rev. Fluid Mech.* **6**, 37-54.
- [57] Willcocks BT, Esler JG. 2012. Nonlinear baroclinic equilibration in the presence of Ekman friction. *J. Phys. Oceanogr.* **42**, 225–242.
- [58] Yakubovich VA, Starzhinskii VM. 1975. *Linear Differential Equations with Periodic Coefficients*, vols. 1 and 2. New York: Wiley.
- [59] Yih C.-S. 1961. Dual role of viscosity in the instability of revolving fluids of variable density. *Phys. Fluids* **4**(7), 806–811.
- [60] Ziegler H. 1952. Die Stabilitätskriterien der Elastomechanik. *Archive Appl. Mech.* **20**, 49–56.